SYNTHESIS, CHARACTERISATION, AND CRYSTALLOGRAPHIC STUDIES OF SULFATHIAZOLE SALTS AND RELATED SPECIES

SITI AINA MARDIA AKHMAD AZNAN

FACULTY OF SCIENCE
UNIVERSITY OF MALAYA
KUALA LUMPUR

2018

SYNTHESIS, CHARACTERISATION, AND CRYSTALLOGRAPHIC STUDIES OF SULFATHIAZOLE SALTS AND RELATED SPECIES

SITI AINA MARDIA AKHMAD AZNAN

DISSERTATION SUBMITTED IN FULFILMENT OF THE REQUIREMENTS FOR THE DEGREE OF MASTER OF SCIENCE

DEPARTMENT OF CHEMISTRY
FACULTY OF SCIENCE
UNIVERSITY OF MALAYA
KUALA LUMPUR

2018

UNIVERSITY OF MALAYA

ORIGINAL LITERARY WORK DECLARATION

Name of Candidate: Siti Aina Mardia Binti Akhmad Aznan

Registration/Matric No: SGR120117

Name of Degree: Master of Science (Research and Dissertation)

Title of Project Paper/Research Report/Dissertation/Thesis ("this Work"):

Synthesis, Characterisation, and Crystallographic Studies of Sulfathiazole Salts and Related Species.

Field of Study:

I do solemnly and sincerely declare that:

(1) I am the sole author/writer of this Work;
(2) This Work is original;
(3) Any use of any work in which copyright exists was done by way of fair dealing and for permitted purposes and any excerpt or extract from, or reference to or reproduction of any copyright work has been disclosed expressly and sufficiently and the title of the Work and its authorship have been acknowledged in this Work;
(4) I do not have any actual knowledge nor do I ought reasonably to know that the making of this work constitutes an infringement of any copyright work;
(5) I hereby assign all and every rights in the copyright to this Work to the University of Malaya ("UM"), who henceforth shall be owner of the copyright in this Work and that any reproduction or use in any form or by any means whatsoever is prohibited without the written consent of UM having been first had and obtained;
(6) I am fully aware that if in the course of making this Work I have infringed any copyright whether intentionally or otherwise, I may be subject to legal action or any other action as may be determined by UM.

Candidate's Signature Date:

Subscribed and solemnly declared before,

Witness's Signature Date:

Name:

Designation:

SYNTHESIS, CHARACTERISATION, AND CRYSTALLOGRAPHIC STUDIES OF SULFATHIAZOLE SALTS AND RELATED SPECIES

ABSTRACT

Co-crystallisation of equimolar quantities of sulfathiazole (STL) with each of 1,4-diazabicyclo[2.2.2]octane (DABCO) and piperazine (PIP) resulted in facile formation of salts [DABCOH][STL_H] (**1**) and [PIPH][STL_H] (**2**), respectively. Crystallographic studies show the formation of aniline-N–H...O(sulfonyl) hydrogen bonds between anions to form supramolecular undulating and zigzag layers, respectively, with the cations being connected to these by charge-assisted N–H...N(thioazole) interactions. The salts formations were confirmed by ^{1}H NMR, IR, Raman spectroscopies, CHN elemental analysis, Single Crystal X-ray Diffraction (SCXRD), Powder X-ray Diffraction (PXRD) and Differential Scanning Calorimetry (DSC) as well as melting point. Solid state grinding competition experiments were monitored by PXRD. In a sequence of experiments where STL was co-ground with a molar equivalent of PIP and *n* equivalents of DABCO (with *n* increasing from 0.1 to 1.0 in 0.1 increments), formation of salt **1** was observed. In related experiments where salt **2** was ground with an equimolar amount of DABCO, substitution of $PIPH^{+}$ by $DABCOH^{+}$ was evident, *i.e.*, postsynthetic metathesis had occurred to about 70% for dry grinding. Quantitative yields were obtained in the case of liquid-assisted grinding (LAG) with a few drops of ethanol after 1.4 equivalents of DABCO were added. These observations are primarily correlated with differences in aniline-N–H...O(sulfonyl) hydrogen bonding that sustain the layers.

Keywords: Crystallographic study, sulfathiazole salt and postsynthetic metathesis.

SINTESIS, PENCIRIAN, DAN KAJIAN KRISTALOGRAFI KE ATAS GARAM SULFATIAZOLA DAN SPESIES YANG BERKAITAN

ABSTRAK

Penghabluran bersama antara sulfatiozola (STL) dan 1,4-diazabisiklo[2.2.2]oktana (DABCO) serta piperazina (PIP) dalam kuantiti mol yang sama menghasilkan garam [DABCOH][STL_H] (**1**) dan [PIPH][STL_H] (**2**). Kajian pembelauan sinar-X menunjukkan pembentukan ikatan hidrogen antara anilina-N–H...O(sulfonil) dengan anion menghasilkan 'supramolekul' yang beralun serta jalinan kation melalui interaksi antara N–H...N(tiazola) membentuk lapisan zig-zag. Analisis ^{1}H NMR, IR, Raman spektroskopi, Analisis unsur CHN, Pembelauan Hablur Tunggal Sinar-X (SCXRD), Pembelauan Serbuk Sinar-X (PXRD), Pengimbasan Pembezaan Kalorimeter (DSC) serta takat lebur mengesahkan pembentukan garam **1** dan **2**. Experimen persaingan bagi kisaran keadaan pepejal dipantau menggunakan PXRD. Eksperimen yang seterusnya, STL telah dikisar dengan kemolaran yang sama dengan PIP dan *n* mol DABCO (*n* meningkat dari 0.1 ke 1.0 mol dengan kadar peningkatan 0.1). Pembentukan garam **1** telah dikenalpasti. Dalam kajian selanjutnya, garam **2** telah dikisar dengan kemolaran yang sama dengan DABCO, penukar gantian $PIPH^{+}$ oleh $DABCOH^{+}$ telah diperolehi, *i.e.*, metatesis selepas sintetik telah berlaku sebanyak 70% bagi kisaran kering. Hasil kuantitatif telah diperolehi dengan kisaran bantuan cecair dengan beberapa titis etanol selepas 1.4 kesetaraan DABCO ditambah. Pemerhatian ini dikaitkan dengan perbezaan ikatan hidrogen anilina-N–H...O(sulfonil) yang menyokong lapisan.

Kata kunci: Kajian kristalografi, garam sulfatiazola dan metatesis selepas sintetik.

ACKNOWLEDGEMENTS

I would like to express my greatest appreciation towards my supervisors, Prof. Dr. Edward Richard Tom Tiekink and Prof. Dr Zanariah Abdullah for their inspiring suggestions, valuable guidance and advice during the course of my research work.

Then, I would like to thank staff members of the Department of Chemistry, Faculty of Science for their kind assistance in various ways in facilitating my research.

Not to forget, my sincere gratitude to all my colleagues who helped me in one way or another and deepest appreciation to them especially the members of my group for being such wonderful, understanding and supportive friends.

I would like to thank the University of Malaya for the research grants of UMRG RG125/10AFR, High Impact Research MoE Grants UM.C/625/1/HIR/MoE/SC/03 and UM.C/625/1/HIR/MoE/SC/12 from the Ministry of Higher Education, Malaysia for financial assistance throughout the entire course.

Last but not least, I would like to dedicate this work to my beloved family especially my parents and my husband who have given me an enormous amount of support and encouragement throughout my whole education and for their continuous belief in me.

TABLE OF CONTENTS

LIST OF FIGURES

LIST OF TABLES

LIST OF SYMBOLS AND ABBREVIATIONS

APIs	:	Active Pharmaceutical Ingredients
^{o}C	:	Degree Celsius
$CDCl_3$	:	Deuterated Chloroform
CHN Elemental Analysis	:	Carbon, Hydrogen and Nitrogen Elemental Analysis
δ	:	Chemical Shift
DMSO-d_6	:	Deuterated Dimethylsulfoxide
DABCO	:	1-Azonia-4-azabicyclo(2.2.2)octane
FT-IR	:	Fourier Transform Infrared
J	:	Coupling Constant
kcal/mol	:	Kilocalorie per mole
LAG	:	Liquid Assisted Grinding
M	:	Molar
m	:	Multiplet
mL	:	Mililitre
mmol	:	Milimoles
NMR	:	Nuclear Magnetic Resonance
PIP	:	Piperazine
s	:	Singlet
Salt **1**	:	[DABCOH][STL_H] Salt
Salt **2**	:	[PIPH][STL_H] Salt
STL	:	Sulfathiazole
t	:	Triplet
v	:	Stretching Vibration

LIST OF APPENDICES

CHAPTER 1: INTRODUCTION

1.1 Crystal Engineering

Organic chemistry has long since evolved from its traditional synthetic chemistry to the now contemporary research in crystal engineering, mostly driven by its relevance in pharmaceutical industries, optical materials and materials science. The most precise definition of crystal engineering was suggested by Desiraju, "…the understanding of intermolecular interactions in the content of crystal packing and in the utilization of such understanding in the design of new solids with desired physical and chemical properties." Desiraju (1989).

While both traditional synthetic chemistry and crystal engineering resemble each other in its analysis and synthesis components, the latter predicts and designs new functionalised solids with more reason and imagination by taking preformed molecules with the intention to produce the desired product in a predetermined approach.

1.2 Intermolecular Interactions

The foundation of a crystal structure formed by various intermolecular interactions, that are responsible for crystal assembly, relates to the study of supramolecular chemistry. Hydrogen bonding plays an important role in crystal architecture due to its structural robustness. The very strong negatively-charged hydrogen bond was proven as one of the most superior forces with energy of 15-40 kcal in comparison to other intermolecular interactions as shown in Table 1.1.

Table 1.1: Strength scale of different intermolecular interactions and hydrogen bonds (Nangia, 2010)

Interaction type	Energy (kcal mol^{-1})	Examples
Charge-assisted hydrogen bonds	15-40	O-H···O^-, F-H···F^-
Coordinative bonds	20-45	M-N, M-O
Strong hydrogen bonds	5-15	O-H···O, N-H···O
Weak hydrogen bonds	1-4	C-H···O, O-H···π
van der Waals interactions	0.5-2	CH_3···CH_3,CH_3···Ph
Heteroatom interactions	1-2	N···Cl, I···I, Br···Br
π-stacking	2-10	Ph···Ph, nucleobases

Adapted from (Nangia, 2010)

A molecule's structure in its crystalline form can be altered by introducing a new substance which may generate more stable crystal packing. This "supramolecular synthesis" approach may be achieved with several attempts. However, it is noted that mechanical grinding has been the most popular and efficient method thus far (Trask *et al*., 2004).

1.3 Mechanochemistry

The grinding of a solid is the form of mechanochemistry that has been used for many years. Chemical reaction transformation is achieved by mechanical forces such as grinding, milling processes and sonication. These techniques can be solvent free and less energy consuming than standard solution reactions. It is a sustainable alternative to conventional solution based and solvothermal chemical processes which impose wastage of solvents in both lab and industry. Hence, mechanochemistry is known as a clean and green technology for future practice.

In this study, co-crystals were produced by solid state grinding. Solvent drop grinding was used as an alternative method to improve the conversion and enhance the kinetics of the desired co-crystal formation. Co-crystals can be defined as quoted from (Aakeröy & Salmon, 2005),

"Only compounds constructed from discrete neutral molecular species can be considered as co-crystal. Consequently, all solids containing ions including complex transition metal ions are excluded. Only co-crystals made from reactants that are solids at ambient conditions were included (Boese *et al*., 2003). A co-crystal is a structurally homogeneous crystalline material that contains two or more neutral building blocks that are present in definite stoichiometric amounts. Based on these definitions, we are essentially left with two families of compounds: binary donor-acceptor complexes and hydrogen bonded co-crystals."

1.4 Co-crystal in Pharmaceutical Industry

In the field of pharmaceutical development, a pure drug crystal property can be enhanced by modifying a pharmaceutical co-crystal that contains a single active pharmaceutical ingredient (API) and a relevant co-former combination.

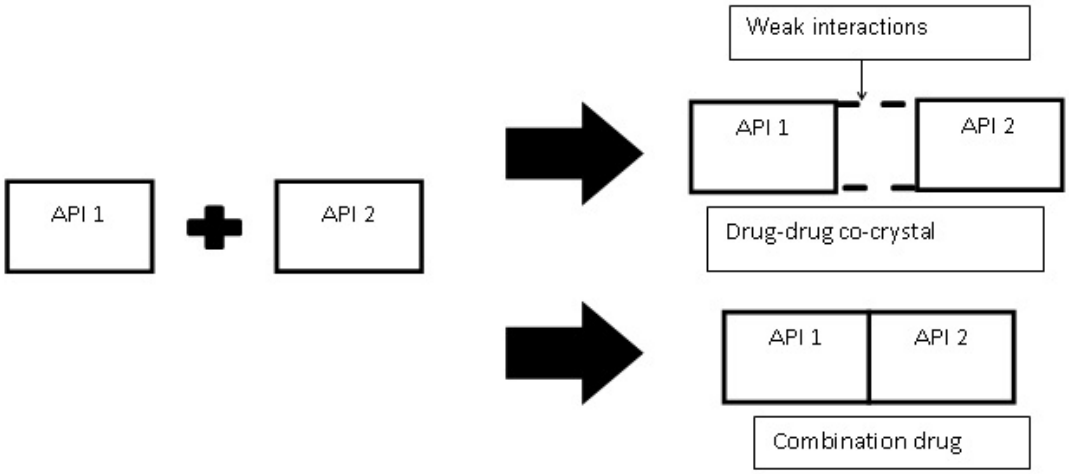

Figure 1.1: Representation of drug-drug co-crystal and combination drug.
(Sekhon, 2012)

1.5 Why Sulfathiazole?

In the realm of the organic solid state, the study of postsynthetic metathesis was done by Caira, Nassimbeni and Wildervank, (Caira *et al*., 1995). In the study, the sulfa drug sulfadimidine–2-hydroxybenzoic acid was formed from co-crystallisation of sulfadimidine and 2-hydroxybenzoic acid. The sample later on, was ground with a stoichiometric amount of 2-aminobenzoic acid producing a new 1:1 co-crystal, sulfadimidine–2-aminobenzoic acid (Caira *et al*., 1995).

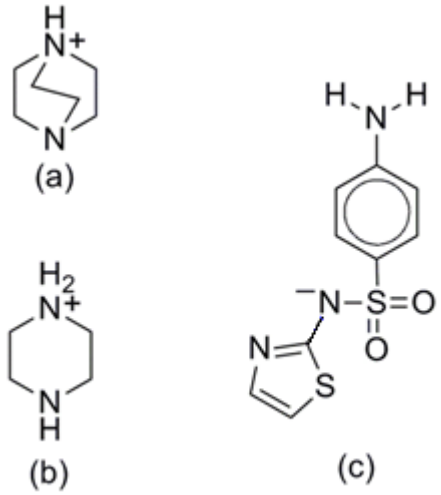

Figure 1.2: Chemical structures of $DABCOH^+$, $PIPH^+$ and STL_H^-

a. 1-azonia-4-azabicyclo(2.2.2)octane cation ($DABCOH^+$)

b. piperazinium cation ($PIPH^+$)

c. 4-aminophenylsulfonyl(1,3-thiazol-2-yl)azanide anion (STL_H^-)

Due to its well-known anti-microbial activity and its five solvent free polymorphs, sulfa drug sulfathiazole, Figure 1.2(c) has captured the attention of most crystal engineers. (Drebushchak *et al*., 2008; Gelbrich *et al*., 2008; Grove & Keenan, 1941; Parmar *et al*., 2007). Sulfathiazole has also attracted the attention of crystal engineers to further a deeper understanding of characterising, controlling and imitate the formation of this sulfa drug (Hu *et al*., 2013; Kelleher *et al*., 2006; Lawrence *et al*., 2010; McArdle

et al., 2010; Munroe *et al*., 2014; Munroe *et al*., 2012; Munroe *et al*., 2011; Sovago, *et al*., 2014). The effectiveness of integrating solvent in the crystal structures of sulfathiazole has been proved by the discovery of more than one hundred solvates of sulfathiazole.

Sulfathiazole along with other sulfa-drugs are well known to form co-crystals (Caira, 2007). In the early days, sulfathiazole was featured prominently as pharmaceutically inspired co-crystals (Stahly, 2009). Sulfathiazole was co-crystallised with proflavin with equimolar proportions 1:1 and it was found in Flavazole® (Mcintosh *et al*., 1945). However, the wide usage of antibiotics and the growing of microbial resistance, the once highly successful sulfa drugs are now becoming ineffective (Wright *et al*., 2014). In the area of developing "new forms of old drugs" to improve effectiveness, driven by crystal engineering strategies (Almarsson & Zaworotko, 2004; Schultheiss & Newman, 2009; Shan & Zaworotko, 2008), this subject of study attracts the attention of the medicinal chemistry (Elder *et al*., 2013; Friščić & Jones, 2010; Kawakami, 2012; Stahl & Wermuth, 2002; Tilborg *et al*., 2014) and crystal engineering communities (Aakeröy *et al*., 2014; Chierotti *et al*., 2013; Goud *et al*., 2014; Maddileti *et al*., 2014; Moradiya *et al*., 2013). The experiment of 1:1 salt formation between sulfathiazole and each of 1,4-diazabicyclo[2.2.2]octane (DABCO) and piperazine, which will form salt **1** and salt **2** respectively, will be reported in this document. Other interesting topic which will be documented is the conversion of salt **2** to salt **1** by grinding salt **2** with DABCO showing that postsynthetic metathesis can also be applicable in the solid state synthesis of organic salts *via* mechanochemistry. Although the challenge of producing salt **1** and **2** is quite significant, but yet it will be proved producible once the results are reported in this document.

1.6 X-ray Crystallography

1.6.1 Single Crystal X-ray Diffraction

Single X-ray diffraction is a non-destructive technique which can reveal the information of the arrangement and architecture of atoms or ions within the crystals. After the discovery of X-rays in the early 1890's, its relevance in the field of chemistry was noted when it was found that X-ray could be diffracted by crystals. A three-dimensional architecture of atoms of a crystal was first achieved *via* X-ray diffraction in 1913 by William Lawrence Bragg. He found X-ray diffraction of sodium chloride crystal "each sodium is surrounded by six equidistant chlorines and each chlorine by six equidistant sodiums". From his findings he infers that sodium chloride crystal consists of sodium ions, chloride ions and no discrete non-charge atoms of sodium and chloride were found (Glusker & Trueblood, 2010).

Subsequently, Katherine Lonsdale was able to demonstrate that the benzene ring is a flat hexagon in which all carbon- carbon double bonds are equal in length and not a ring structure with alternating single and double bonds (Glusker & Trueblood, 2010).

The main purpose of performing crystal structure analysis by using X-ray or neutron diffraction is to obtain detail information about the positions of individual atoms at the atomic level in a 3-dimensional picture. The detailed information includes interatomic distances, bond angles, planarity of a particular group of atoms, the angle between planes, conformation at detail around bonds, information about molecular packing, molecular motion in the crystal and molecular charge distribution.

1.6.2 Powder X-ray Diffraction

"Finger print identification" of numerous solid materials e.g. asbestos, quartz etc. are always correlated with their powder diffraction patterns. In powder or polycrystalline diffraction, it is important to have a sample with a smooth plane. The sample has to be

ground down to fine particles of about 0.002 mm to 0.005 mm cross section. The ideal sample is homogeneous and the crystallites are randomly orientated and to have a smooth flat surface, the sample is pressed into a sample holder. The solid fine particles are randomly distributed exposing all possible h, k, l planes. Only crystallites having reflecting planes (h, k, l) parallel to the specimen's surface will contribute to the reflected intensities.

1.6.3 Diffraction Patterns

Goniometer configuration is determined by a diffraction pattern that consist of a plot of reflected intensities versus the detector angle 2-theta (theta). Values of the 2-theta for each peak can be calculated based on the wavelength of anode material used. Thus, it is important to minimise the peak position to the interplanar spacing d which is correlated to the h,k,l planes that generate the reflection event. The value of d-spacing will be determined by the metrics of the unit cell. According to Bragg's law, a simple relation for scattering angles can be calculated using $2d_{hkl} \sin \theta = n\lambda$. Hence, the dimension of the unit cell can be resolved when the intensity (area under the peak) and the indices h, k, l are known.

1.7 Crystal

"A crystal is defined as a solid that contains a very high degree of long-range three-dimensional internal order of the component atoms, molecules or ions. Many studies were conducted since early times, mostly with regards to the external features of crystals" (Glusker & Trueblood, 2010).

However, it was Max von Laue who noticed that periodic internal organization of crystals were able to diffract electromagnetic radiation of specific wavelength and he was able to reason the distances between atoms or ions in details. A crystal's ability to diffract was demonstrated in an experiment which also revealed that X-rays have wave-like properties (Glusker & Trueblood, 2010).

Even though it's external appearance is of flat faces and straight edges seems like the most obvious property of a crystal, this is not necessary or sufficient to define a crystal, rather it is internal order and it's regular internal repetition quality. This was first suggested by Johanes Kepler and some of the earliest pictures of crystals viewed under microscope were published by Robert Hooke (Glusker & Trueblood, 2010).

Crystallisation can be achieved through many methods, most often from solution. The steps to obtain crystals include saturation of solution, supersaturation. The most crucial event is nucleation, where solute molecules meet in solution and form small aggregates. More molecules are then laid out on the nucleus surface and eventually a crystal forms. All crystals are built up of periodic three-dimensional translational repetition of some basic structural pattern. This basic component is called "unit cell".

1.8 Objectives of Studies

The objectives of this research were:

- To synthesise and to study the correlations between molecular structure, crystal packing and physical properties of the selected salts derived from Sulfathiazole.
- To study if crystal packing efficiency is valid to be used as a benchmark for stability of a compound.
- To prove that LAG (Liquid Assisted Grinding) can be used to improve the conversion of one compound (salt) into another.

CHAPTER 2: EXPERIMENTAL

2.1 Chemicals

Piperazine and sulfathiazole, 1,4-diazabicyclo[2.2.2]octane were purchased as analytical grade from Merck and were used throughout the entire experiment . All solvents and reagents were commercially available and used as obtained without further purification unless otherwise stated.

2.2 Spectroscopic Analyses

2.2.1 ^{1}H NMR Spectroscopic Analysis

For ^{1}H spectroscopic analysis, machines that were used include a Varian Inova^{TM} 500 NMR spectrometer performing at 500 MHz and JEOL, ECA 400 MHz NMR spectrometer performing at 400 MHz. All of the NMR samples were prepared by adding 20–30 mg of the respective sample to 1 mL of DMSO-d_6. The NMR spectras were recorded in DMSO-d_6 at 25 °C, using the DMSO residual proton at δ 2.49 as the internal standard. Chemical shifts are reported in ppm on the δ scale and coupling constants are given in Hz.

2.2.2 Infrared Spectroscopy

IR spectra in the range 4000 - 450 cm^{-1} were obtained by the Attenuated Total Reflectance (ATR) technique on a Perkin Elmer RX1 FTIR spectrophotometer.

2.2.3 Raman Spectroscopic Analysis

Bruker Vector22 spectrophotometer in the range 4000 - 400 cm^{-1} was used to measure raman scattering. Measurements were made at room temperature under ambient conditions using a microscope objective to focus the incident laser light upon individual grains. Excitation at 632.8 nm or 514.5 nm was used and no resonance effects were observed. For easier comparison amongst spectra, the data presented have

been normalised and the background was subtracted by *L. E. McNeil from Department of Physics and Astronomy, University of North Carolina*.

2.2.4 Melting Point Determination

Krüss KSP1N melting point apparatus was used to determine the melting point using glass capillaries and were uncorrected.

2.2.5 CHN Elemental Analysis

The carbon, hydrogen and nitrogen elemental compositions of samples from this work were obtained from a Perkin-Elmer PE 2400 CHN Elemental Analyser.

2.2.6 DSC Analysis

In the range between 30–400 °C at the rate of 10 °C/min, differential scanning calorimetric data were recorded with a Perkin Elmer DSC 6 using a T_{zero} aluminium pan.

2.3 X-ray Crystallography

Rigaku AFC12/SATURN724 diffractometer fitted with MoKα radiation (λ = 0.71073 Å) so that θ_{max} was 27.5° was used to measure the intensity data for colourless crystals of salt **1** and yellow salt **2**. The measurement was done at 98 K and data processing was performed with CrystalClear (Rigaku/MSC inc., 2004), while the absorption correction applied to the data of salt **2** was with ABSCOR (Higashi, 1995).

2.4 PXRD Analysis

PANalytical Empyrean XRD system with Cu-Kα1 radiation (λ= 1.54056 Å) in the 2θ range 5 - 90^{o} with a slit size = 0.4785° was used to record powder X-ray diffraction. Data were recorded with a comparison between experimental and calculated (from CIF's) PXRD patterns. The software used for powder X-ray diffraction was X'PertHighScore Plus (Almelo, 2009).

2.5 Synthesis of Salts

2.5.1 Preparation of Salts

All reactions were carried out under ambient conditions.

Salt **1**, [DABCOH][STL_H]

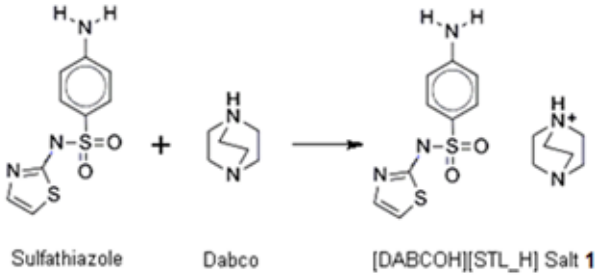

Figure 2.1: Preparation of Salt **1**

In 50 mL of methanol, sulfathiazole (4.5 mmol, 1.14 g) and 1,4-diazabicyclo[2.2.2]octane, DABCO (4.5 mmol, 0.50 g) were dissolved and heated at 70 °C. Water (20 mL) was added while heating. After 2 hours of stirring, the resulting mixture produced a clear solution. The solution was left for slow evaporation at room temperature and after a week yielding colourless crystals. The yield was 0.8 g (89 %). Analytical calculation for salt **1** ($C_{15}H_{21}N_5O_2S_2$): C, 49.02; H, 5.76; N, 19.06. Found: C, 49.03; H, 5.90; N, 19.04. The melting point was 180 °C. Results for ^{1}H NMR, IR, Raman, PXRD, SCXRD and DSC are in the discussion section.

Salt **2,** [PIPH][STL_H]

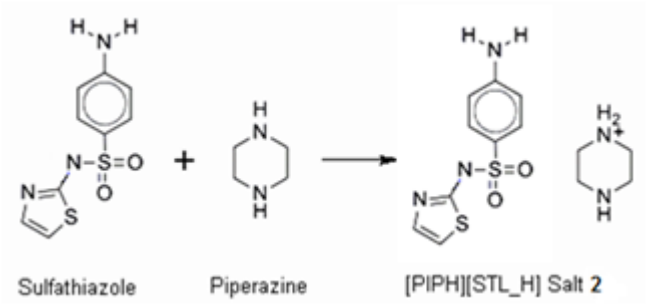

Figure 2.2: Preparation of Salt **2**

In 50 mL of acetone, sulfathiazole (13.9 mmol, 3.55 g) and piperazine (13.9 mmol, 1.20 g) were dissolved and heated with stirring at 70 °C for 2 hours. After a week of slow evaporation at room temperature, 1.85 g (87 %) of yellow crystals formed. Analytical calculation for salt **2** ($C_{13}H_{19}N_5O_2S_2$): C, 45.73; H, 5.61; N, 20.51. Found: C, 45.44; H, 5.44; N, 20.03%. The melting point of the crystals was ranging from 176–178 °C. Results for ^{1}H NMR, IR, Raman, PXRD, SCXRD and DSC are in the discussion section.

2.6 Preparation for Metathesis Experiments

DABCO of (0.1 molar equivalents, 0.004 g) was ground with crystals of salt **2** (0.122 g) using a mortar and pestle. Additional experiments of dry grinding were conducted in 0.1 molar equivalent increments to a maximum of 1.5. The dry grinding procedure was carried out for at least 5 min followed by measurement with PXRD. LAG experiments were also conducted with 1.1–1.5 molar equivalents of DABCO addition by using ethanol as the solvent. For competition experiments, STL (1.95 mmol, 0.50 g) and PIP (1.95 mmol, 0.169 g) were ground together for 5 min with addition of 0.1 molar equivalent (0.022 g) of DABCO using a mortar and pestle. The rest of the experiments were carried out similarly with 0.1 molar equivalent increments.

2.7 X-ray Crystallography Studies

The structures were solved by direct methods (Sheldrick, 2008), and full-matrix least squares refinement was performed on F^2 with anisotropic displacement parameters for all non-hydrogen atoms (Sheldrick, 2008). The O- and N-bound hydrogen atoms were located from difference maps and were refined with O–H = 0.84±0.01 Å and N–H = 0.88-0.92±0.01 Å; the C-bound hydrogen atoms were included in the refinement in their idealized positions. A weighting scheme of the form $w = 1/[\sigma^2(F_o^2) + (aP)^2 + bP]$ where $P = (F_o^2 + 2F_c^2)/3$ was introduced in each case. The absolute structures of each of crystal salt **1** and **2** were determined on the basis of difference in Friedel pairs included in their respective data sets as confirmed by the values of the Flack parameters (Flack, 1983), *i.e.*, -0.02(7) and 0.06(5) for salt **1** and **2**, respectively. The programs WinGX (Farrugia, 2012), PLATON (Spek, 2003), ORTEP-3 for Windows (Farrugia, 2012), and DIAMOND were also used in the study.

CHAPTER 3: RESULTS AND DISCUSSION

3.1 Synthesis and Characterisation

Co-crystalisation experiments between sulfathiazole (STL) and each of 1,4-diazabicyclo[2.2.2.]octane (DABCO) and piperazine (PIP), formed crystal salts **1** and **2**, respectively, as shown in Figures 2.1 and 2.2.

The ^{1}H NMR spectra conducted in DMSO-d_6 solution for 1:1 ratios of the respective pairs of co-formers clearly indicated salt formation as shown in Table 3.1. The absence of the thiazole-H resonance observed in STL, indicated that proton transfer from sulfathiazole had occurred. Upfield shifts were noted for all remaining protons within thiazole ring. Full structural characterisation of salt was achieved through X-ray crystallography.

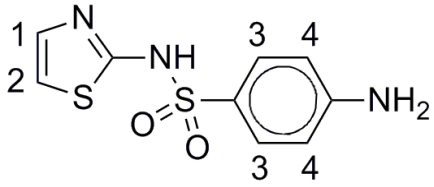

Table 3.1: ^{1}H NMR data sulfathiazole (STL) and 4-aminophenylsulfonyl-(1,3-thiazol-2-yl)azanide anion (STL_H^{-}), anions in Salts **1** and **2**

H	STL (ppm)	Salt 1 (ppm)	Salt 2 (ppm)
thiazole-H	12.37	-	-
aniline-H	5.82	5.67	5.53
1	7.14	7.08	6.98
2	6.70	6.61	6.49
3	7.39	7.40	7.41
4	6.52	6.51	6.48

Given the solid-state observations and the facile formation of salts in solution, it was thought worthwhile to perform competition experiments in DMSO-d_6 solution monitored by ^{1}H NMR, see Table 3.1 for data. The methylene resonance for pure DABCO occurred as a sharp singlet at δ 2.69 ppm and upon proton transfer from STL in a solution containing a 1:1 stoichiometric mixture this resonance shifted downfield to δ 2.71 ppm. The comparable δ values for PIP/$PIPH^+$ were 2.48 and 2.87 ppm, respectively. In a separate NMR experiment, from Table 3.2, DMSO-d_6 solution containing a 1:1:1 molar ratio of STL, DABCO and PIP featured two sharp resonances at 2.85 and 2.66 ppm with an integration ratio of 2 to 3, indicating preferential protonation of PIP over DABCO. This observation is in accord with expectation in that PIP is more basic than DABCO as seen for example in the calculated ("Advanced Chemistry Development (ACD/Laboratories)," 2014) *p*Ka values of 9.55±0.10 and 8.19±0.10, respectively, an observation correlated with steric pressures in DABCO and tertiary amines in general. This suggests that the substitution of $PIPH^+$ in salt **2** by $DABCOH^+$ leading to salt **1** is due to solid-state considerations.

Table 3.2: ^{1}H NMR data of DABCO, PIP, Salt **1**, Salt **2** and STL, DABCO and PIP

Solution containing	**δ**	**Assignment**
DABCO	2.69	methylene-H in DABCO
PIP	2.48	methylene-H in PIP
1	2.71	methylene-H in $DABCOH^+$
2	2.87	methylene-H in $PIPH^+$
STL, DABCO and PIP	2.85	methylene-H in $PIPH^+$; integration = 8.35 = 8
	2.66	methylene-H in DABCO; integration = 11.72 = 12

3.2 Infrared and Raman Spectroscopy

Another analysis that has proven useful in distinguishing between co-crystal/salt formation is Raman spectroscopy (Brittain, 2009; Roy *et al.*, 2013). The most impressive finding from the Raman measurements in the present study was that the spectra recorded from the crystals grown from a solution containing the two constituents and from the crystals prepared by grinding the constituent powders together are virtually identical, apart from some minor variations in relative intensity which may be due to variations in the orientation of the individual crystallites from which the measurements were made. These spectra differed significantly from those of the precursor molecules as shown in Figures 3.1 and 3.2. Peaks observed at 513 and 1269 cm^{-1} in the spectrum of the crystals produced by grinding but did not appear in the spectrum of the solution-grown crystals. This agreement between the Raman-active vibrational modes of the two types of crystals clearly shows that the local bonding in the two species is essentially the same, *i.e.* that the two methods of fabrication produce the same crystal structure.

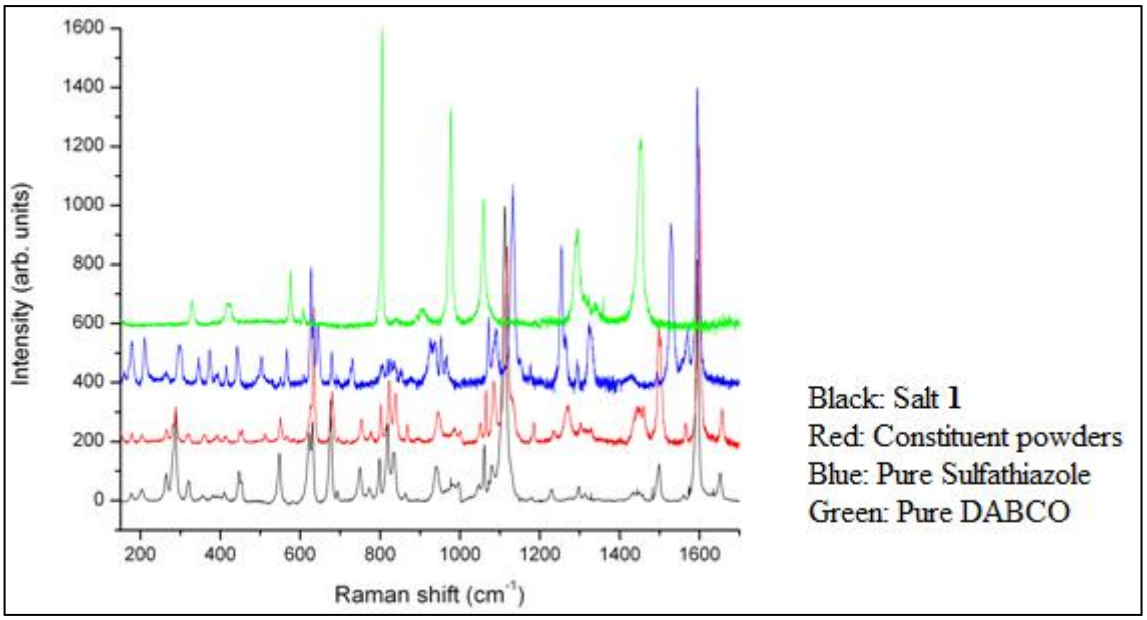

Figure 3.1: Raman spectra for conformers and Salt **1**

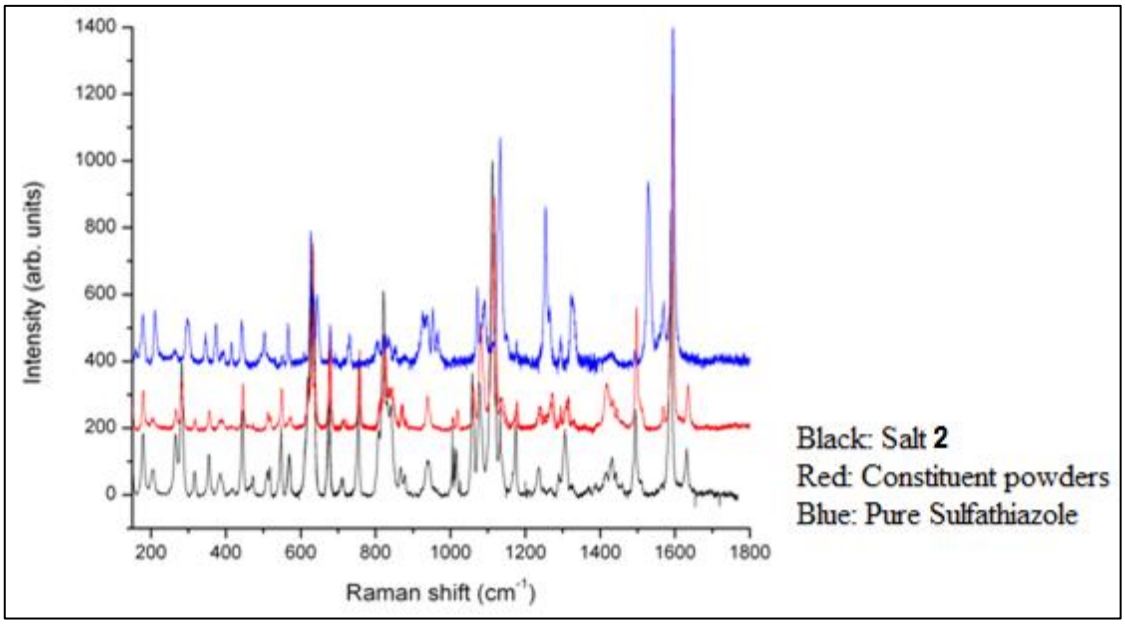

Figure 3.2: Raman spectra for conformers and Salt **2**

From the data tabulated in Table 3.3, it is evident that sulfathiazole exhibits IR bands consistent with those of form III (Hu *et al*., 2010), confirming the conclusions of the PXRD study.

Table 3.3: IR (cm^{-1}) absorption for sulfathiazole (STL) and the 4-aminophenylsulfonyl-(1,3-thiazol-2-yl)azanide, [STL_H^-], anions in Salt **1, 2** and sulfathiazole polymorph form III

Mode	**STL (cm^{-1})**	**Salt 1 (cm^{-1})**	**Salt 2 (cm^{-1})**	**Sulfathiazole polymorph form III (cm^{-1})**
-SO_2N–H	3274	–	–	
-NH_2 (sym)	3317	3352 (+35)	3345 (+28)	3280
-NH_2 (asym)	3350	3412 (+62)	3449 (+99)	3320
-SO_2- (sym)	1131	1121 (-10)	1117 (-14)	1133
-SO_2- (asym)	1322	1320 (-2)	1311 (-11)	1323
C–N	1267	1234 (-33)	1241 (-26)	1530
C–N(thiazole)	1572	1655 (+83)	1635 (+63)	1530
C–S(thiazole)	924	948 (+24)	940 (+16)	1072

[a] The values in parentheses are the corresponding Δν values, *i.e.*, the frequency difference between the same mode of anionic-STL and STL in cm^{-1}, *i.e.*, Δν = ν([STL_H]) - ν(STL).

The most obvious difference in the IR spectra relates to the absence of ν(N–H) at 3274 cm^{-1} in the salts indicating proton transfer had occurred (Figures 3.3 and 3.4).

It is the most explicit difference in the IR spectra that relates to this matter. As for ν(C=N) and ν(C–$N_{thiazole}$), systematic shifts to higher and lower frequency were observed respectively, together with reduced and increased bond orders in the salts according to the corresponding ν(C=N) and ν(C–$N_{thiazole}$) as shown in Table 3.3. At the same time small shifts were noted for $\nu_{sym,\ symm}(SO_2)$, significant shifts are evident for bands due to amino group.

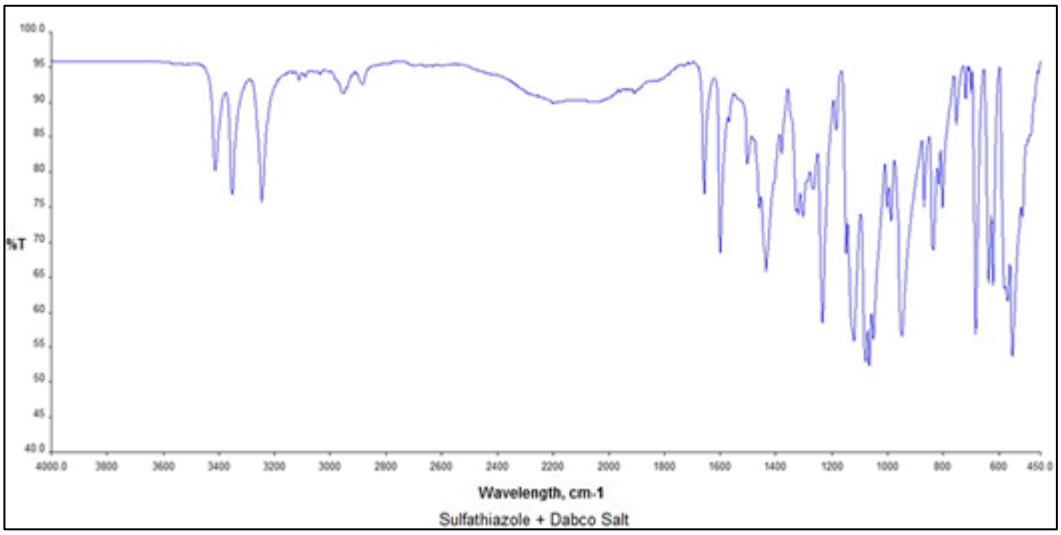

Figure 3.3: IR spectra of Salt **1**

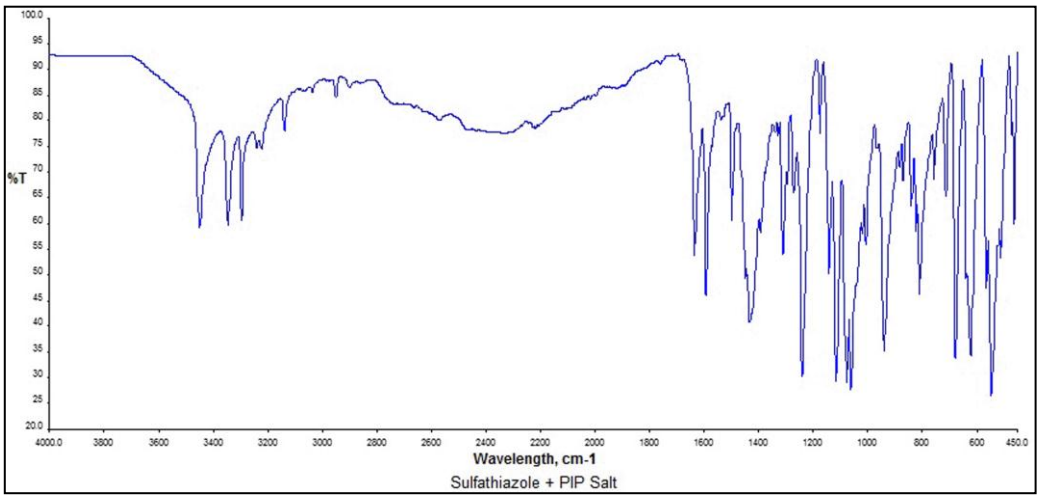

Figure 3.4: IR spectra of Salt **2**

3.3 Single Crystal X-ray Crystallography

The molecular structures of the asymmetric unit of salt **1** contains a 4-aminophenylsulfonyl(1,3-thiazol-2-yl)azanide anion (STL_H^-) and a 1-azonia-4-azabicyclo(2.2.2)octane ($DABCOH^+$) cation (**1)** or a piperazinium ($PIPH^+$) cation (**2**) as shown in Figures 3.5 and 3.6.

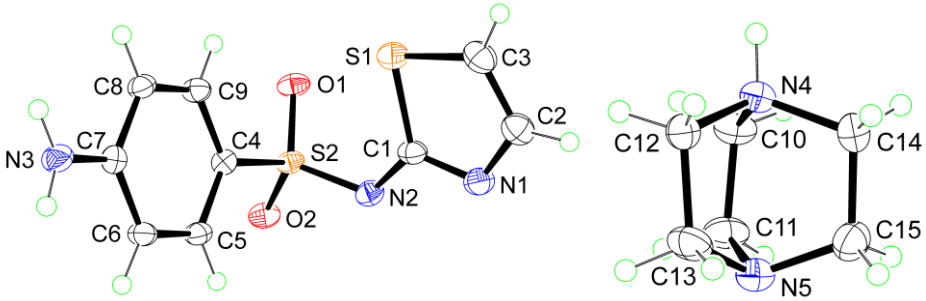

Figure 3.5: Molecular structures and crystallographic numbering for the 4-aminophenylsulfonyl(1,3-thiazol-2-yl)azanide anion and 1-azonia-4- azabicyclo(2.2.2)octane cation in the structure of Salt 1

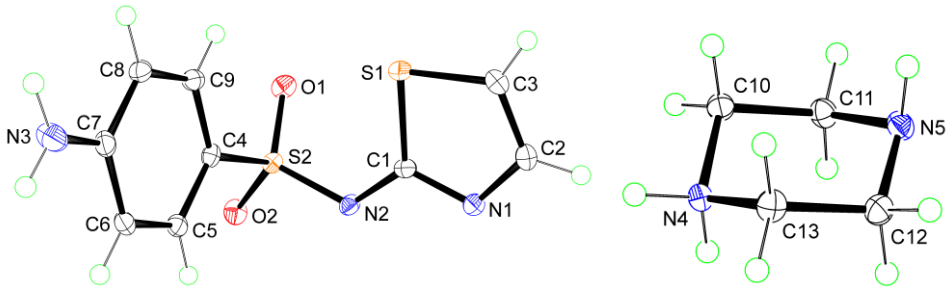

Figure 3.6: Molecular structures and crystallographic numbering for the 4-aminophenylsulfonyl(1,3-thiazol-2-yl)azanide anion and piperazinium cation in the structure of Salt 2

Details of cell data, X-ray data collection, and structure refinement are given in Table 3.4.

Table 3.4: Crystal data and refinement details for Salt **1** and Salt **2**

Parameter	**Salt 1**	**Salt 2**
Formula	$C_4H_{11}N_2$, $C_9H_8N_3O_2S_2$	$C_6H_{13}N_2$, $C_9H_8N_3O_2S_2$
Formula weight	367.49	341.45
Crystal system	orthorhombic	orthorhombic
Space group	$P2_12_12_1$	$P2_12_12_1$
a, Å	15.349(12)	8.4158(16)
b, Å	6.620(5)	10.1810(19)
c, Å	17.148(12)	17.941(4)
V, Å^3	1742(2)	1537.2(5)
Z	4	4
Density, g/cm^3 (calculated)	1.401	1.475
μ/mm^{-1}	0.324	0.361
Reflections collected	13501	5827
Independent reflections	3988	3474
Reflections with $I \geq 2\sigma(I)$	3860	3443
R (observed data)	0.042	0.024
a, *b* in weighting scheme	0.044, 0.285	0.034, 0.418
R_w (all data)	0.109	0.062
Largest diff. peak and hole e Å^{-3}	0.32 and -0.39	0.28 and -0.25
CCDC deposition number	843173	843174

The geometric parameters for salt **1** and **2** match other structurally characterised STL_H anions, and are listed in Table 3.5.

Table 3.5: Selected bond distances (Å) and and angles (°) for [DABCOH][STL_H] (**1**), [PIPH][STL_H] (**2**)

Compound	**Salt 1** ***n* = 0**	**Salt 2** ***n* = 0**
S*n*2-N*n*2	1.586(2)	1.5839(13)
S*n*2-O*n*1	1.4744(18)	1.4549(11)
S*n*2-O*n*2	1.4608(18)	1.4583(11)
C*n*1-S*n*1	1.781(2)	1.7644(14)
C*n*3-S*n*1	1.736(3)	1.7291(15)
C*n*1-N*n*1	1.323(3)	1.3276(18)
C*n*2-N*n*1	1.388(3)	1.3848(18)
C*n*1-N*n*2	1.360(3)	1.3558(18)
C*n*7-N*n*3	1.375(3)	1.370(2)
C*n*2-C*n*3	1.361(4)	1.351(2)
S...O	3.060(3)	3.0295(12)
N...O	-	-
C*n*1-S*n*1-C*n*3	90.11(12)	89.82(7)
O*n*1-S*n*2-O*n*2	114.92(10)	115.42(7)
O*n*1-S*n*2-N*n*2	113.31(11)	113.36(7)
O*n*1-S*n*2-C*n*4	105.64(10)	106.08(7)
O*n*2-S*n*2-N*n*2	106.37(11)	106.03(7)
O*n*2-S*n*2-C*n*4	107.92(11)	106.76(7)
N*n*2-S*n*2-C*n*4	108.43(10)	108.90(7)
C*n*1-N*n*1-C*n*2	112.1(2)	111.48(12)
C*n*1-N*n*2-S*n*2	119.89(16)	120.06(10)
S*n*2-N*n*2-C*n*1-S*n*1	-7.1(3)	1.23(18)
C*n*1-N*n*2-S*n*2-C*n*4	-65.6(2)	-71.25(13)
Dihedral angle between thiazole and aniline rings	89.67(11)	84.83(7)

Due to its notable characteristic of conformational flexibility (Parkin *et al*., 2008) one of the crystallographically characterised sulfonamide STL_H anions, relative orientation of the sulfoxide and thiazole residues enables the formation of an intramolecular S←O interaction (Nakanishi *et al*., 2007), as shown in Figure 2.1. From Table 3.5 the result of these conformational observations is that each STL_H anion adopts an approximate U-shape (the dihedral angles between the five- and six-membered rings are 89.67(11)° and 84.83(7)°), respectively which proves important in determining the crystal packing patterns.

Geometric data denoting the hydrogen bonding and other intermolecular interactions operating in the crystal structures of salt **1** and **2** are collected in Table 3.6 and Table 3.7.

Table 3.6: Summary of intermolecular interactions (A–H…B; Å, º) operating in the crystal structures of Salt **1**

A	**H**	**B**	**H…B**	**A…B**	**A-H…B**	**Symmetry operation**
N3	H1n	O1	2.09(2)	2.945(3)	171(3)	½+*x*, ½-*y*, 1-*z*
N3	H2n	O2	2.138(19)	2.975(3)	158(3)	½+*x*, -½-*y*, 1-*z*
N4	H3n	N1	1.81(2)	2.733(4)	176(3)	*x*, *y*, *z*
C8	H8	O2	2.52	3.461(4)	172	½+*x*, ½-*y*, 1-*z*
C3	H3	Cg(C4-C9)	2.86	3.611(4)	137	1-*x*, ½+*y*, ½-*z*
C10	H10a	Cg(S1,N1,C1-C3)	2.89	3.773(4)	149	*x*, -1+*y*, *z*

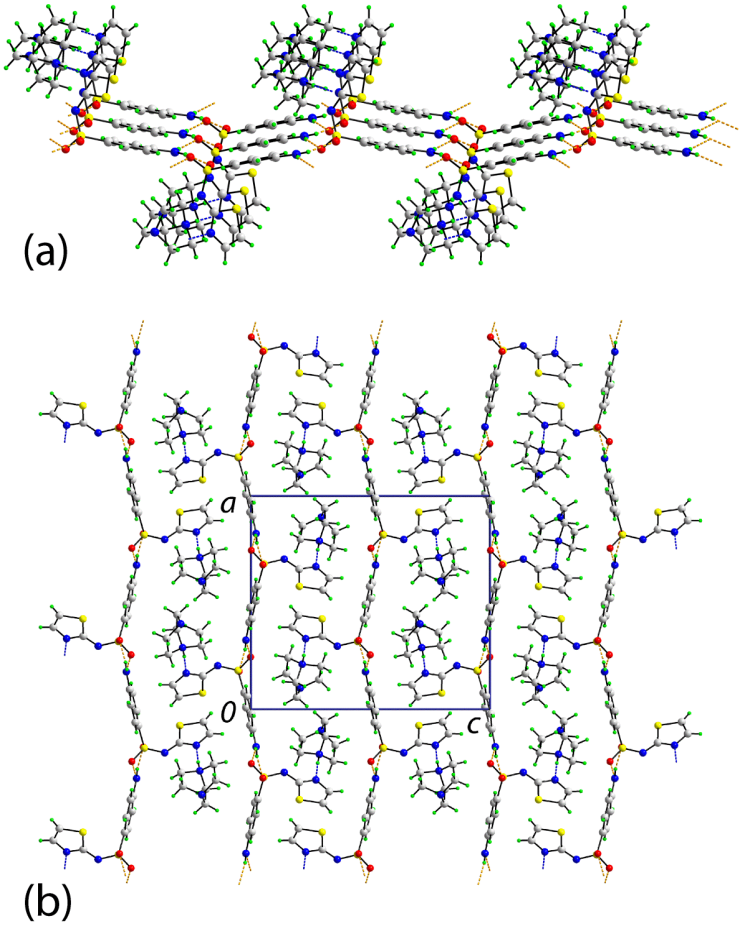

Figure 3.7: View of the crystal packing in Salt **1**

(a) Undulating supramolecular layer comprising anions consolidated by aniline-N–H...O(sulfonyl) hydrogen bonding, shown as orange dashed lines, connected to the cations *via* ammonium-N–H...N(thiazole) hydrogen bonding (blue dashed lines).

(b) Projection down the *b*-axis of the unit cell contents highlighting the interdigitation of layers.

For the crystal structure of salt **1**, the aggregation of anions into undulating layers in the *ab*-plane, *via* aniline-N–H...O(sulfonyl) hydrogen bonds, with the thiazole slits protruding almost in a perpendicular appearance to either side, Figure 3.7. Affiliated with the anionic layers by charge-assisted N–H...N (thiazole) hydrogen bonds are the $DABCOH^+$ cations, Figure 3.7(a). Interdigitate neutral layers were formed along the *c*-axis and it is shown in Figure 3.7(b). Additional stabilisation to this arrangement is supported by phenyl-C_8–H...O_2 interactions. However, neither the azanide-N_2 nor

amine-N_5 atoms form significant intermolecular interactions. The primary interactions between layers are of the type thiazole- and ammonium-C–H... π as indicated in Table 3.6.

Table 3.7: Summary of intermolecular interactions (A–H…B; Å, º) operating in the crystal structures of Salt **2**

A	H	B	H…B	A…B	A-H…B	Symmetry operation
N3	H1n	O2	2.359(13)	3.226(2)	177.4(16)	-*x*, -½+*y*, 1½-*z*
N3	H2n	O2	2.290(15)	3.1436(19)	165.4(14)	-1+*x*, *y*, *z*
N4	H3n	N1	1.817(14)	2.7373(18)	170.3(14)	-½+*x*, ½-*y*, 2-*z*
N4	H4n	N5	1.966(15)	2.8639(19)	163.3(15)	-½+*x*, ½-*y*, 2-*z*
N5	H5n	Cg(S1,N1,C1-C3)	2.503(16)	3.3559(16)	155.5(14)	½+*x*, ½-*y*, 2-*z*
C11	H11b	Cg(C4-C9)	2.50	3.3391(17)	143	½+*x*, ½-*y*, 2-*z*

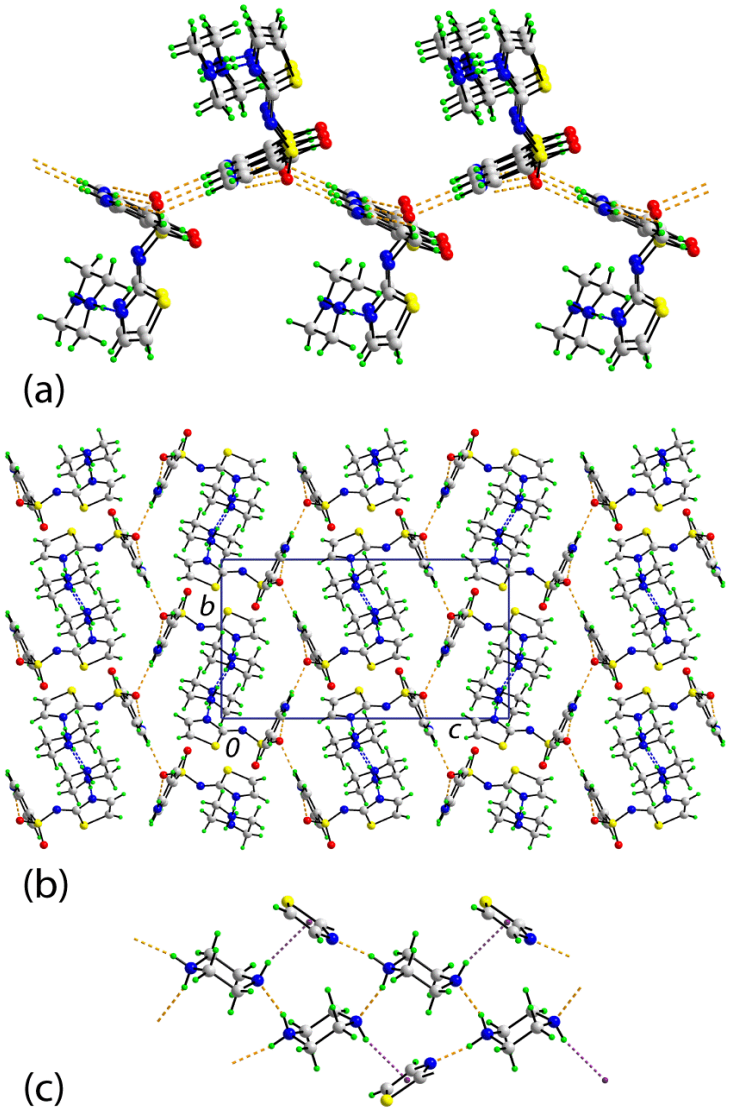

Figure 3.8: View of the crystal packing in Salt **2**

(a) Zigzag supramolecular layer comprising anions consolidated by aniline-N–H...O(sulfonyl) hydrogen bonding, shown as orange dashed lines, connected to the cations *via* ammonium-N–H...N(thiazole) hydrogen bonding (blue dashed lines) which are obscured in this view.

(b) Projection down the *a*-axis of the unit cell contents highlighting the interdigitation of the layers and with connections between cations mediated by ammonium-N–H...N(amine) hydrogen bonding (blue dashed lines).

(c) Supramolecular chain comprising cations connected by ammonium-N–H...N(amine) hydrogen bonding and linked to the anion layers by N–H...π(thiazole) interactions, shown as purple dashed lines.

The supramolecular aggregation in salt **2** on the other hand**,** closely resembles the crystal structure of salt **1**, *ie*. *via* aniline-N–H...O(sulfonyl) hydrogen bonds, the anions aggregate into zig-zag layers. In this case, it involves only one of the sulfonyl-O_2 atoms which is bifurcated; the sulfonyl-O_1 atom forms a close intramolecular C–H...O contact. The cations are associated with the layers as in salt **1**, Figure 3.8(a). The layers inter-digitate along the *c*-axis and associate *via* ammonium-N–H...N(amine) hydrogen bonds, Figure 3.8(b); additional stabilisation to the arrangement from ammonium-C–H...π interactions serve to connect the layers. The residual acidic hydrogen, *i.e*. residing on the amine-N5, forms a relatively rare N–H...π interaction (Coupar *et al*., 1996; Knop *et al*., 1994), as illustrated in Figure 3.8(c).

In terms of hydrogen bonding, a common feature of the crystal structures is the formation of charge assisted cation-N–H...N(thiazole) hydrogen bonds. Both aniline hydrogen atoms participate in aniline-N–H...O(sulfonyl) hydrogen bonding with two different sulfonyl-O atoms in the case of salt **1** but only one sulfonyl-O atom in the structure of salt **2**. An additional conventional hydrogen bond occurs in salt **2**, namely charge assisted N–H...N hydrogen bonds between cations.

3.4 Powder X-ray Diffraction

Powder X-ray diffraction experiments were carried out on STL. It was identified by PXRD as form III (Hu *et al*., 2010) and co-ground with each of DABCO and PIP in order to determine whether the facile salt formation observed in solution can be translated into the solid-state. As can be seen from Figure 3.9 and 3.10, salt **1** and salt **2** were prepared quantitatively in bulk form by dry grinding and were crystallographically characterised.

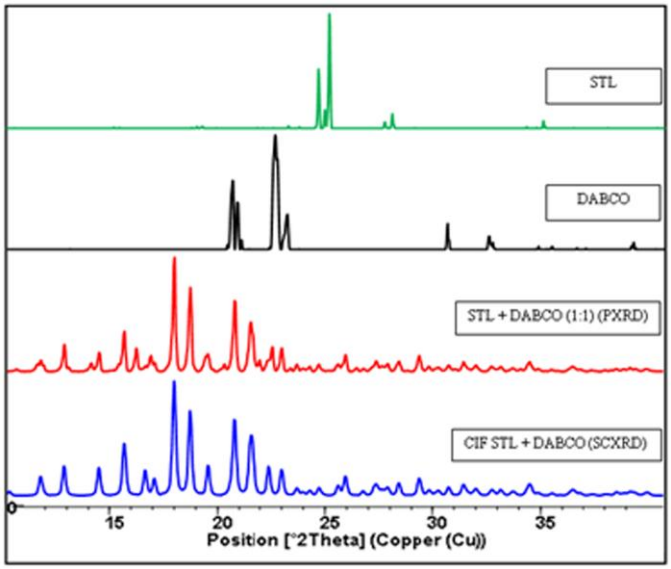

Figure 3.9: PXRD trace of Salt **1**

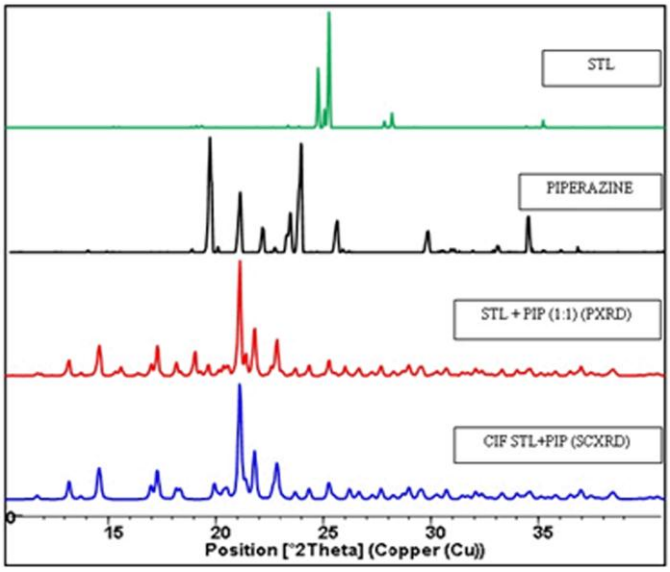

Figure 3.10: PXRD trace of Salt **2**

a. Green trace: Pure sulfathiazole.
b. Black trace: DABCO
c. Red trace: PXRD trace of salt after dry grinding.
d. Blue trace: Calculated PXRD based on the single crystal structure.

From Figure 3.9, it can be concluded that co-crystal salt **1** was formed based on identical trace between the red trace which is PXRD trace salt after dry grinding and the blue trace which was calculated PXRD based on single crystal structure.

On the other hand, Figure 3.10 shows that co-crystal salt **2** was formed from the comparison trace between the red trace (PXRD trace salt after dry grinding) and blue trace (calculated PXRD based on single crystal structure).

3.5 Differential Scanning Calorimetry

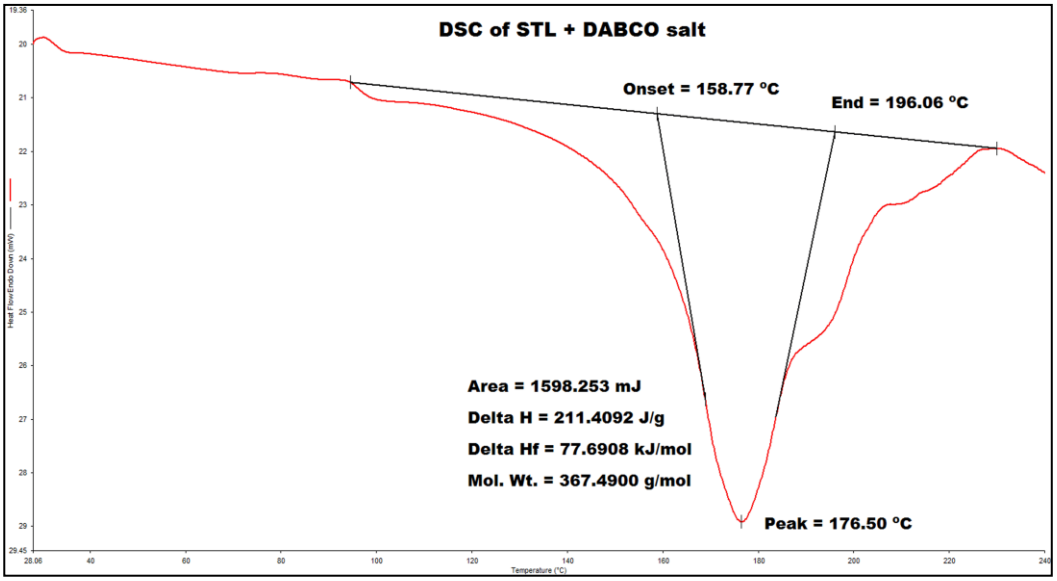

Figure 3.11: DSC trace of Salt **1**

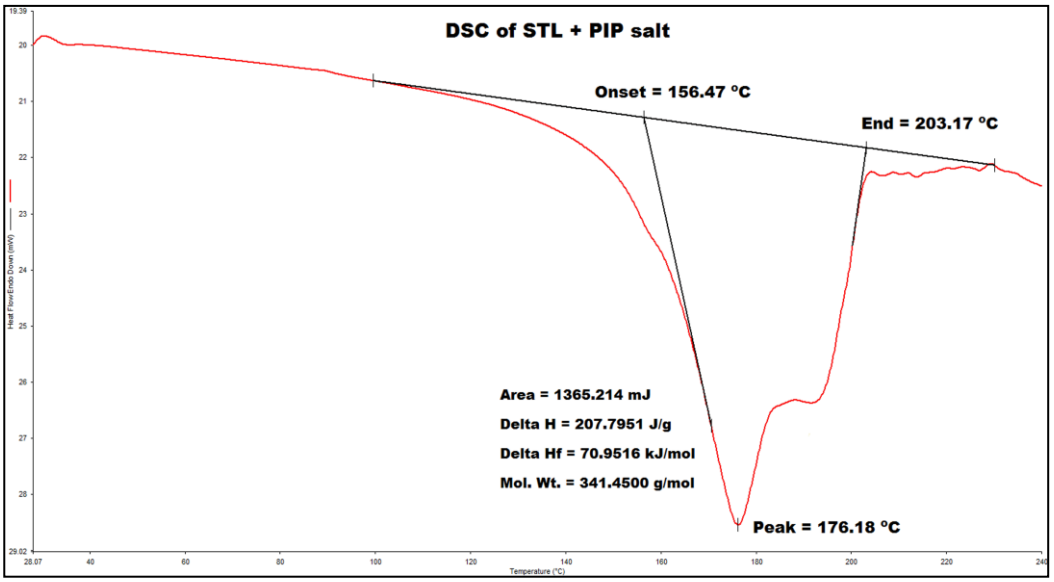

Figure 3.12: DSC trace of Salt **2**

The DSC of salt **1** and **2** were similar, whereby each of them exhibits a significant endothermic peak around 176 °C corresponding to melting as recorded in Figure 3.11 and Figure 3.12. In the case of salt **1**, the endothermic peak was at 176.5 °C with onset and end temperatures of 158.7 and 196.1 °C, respectively, and with $\Delta H_{melting}$ = 77.7 kJ/mol. For salt **2**, the endothermic step was at 176.2 °C (onset-end 156.5-203.2 °C) with $\Delta H_{melting}$ = 71.0 kJ/mol. The progress of the solid state reactions are nicely correlated with the DSC results which showed that $\Delta H_{melting}$ was about 10% higher for salt **1** over salt **2**. However, a consideration of the calculated densities, *i.e*. 1.401 g/cm^3 for salt **1** and 1.475 g/cm^3 for salt **2** suggests that salt **2** might be the more compact structure, although an elongation of the c-axis in salt **2** compare to salt **1**, the axis along which layers stack, has already been noted. The reduced proportion of hydrogen bonds in salt 2 probably contributes to the lower $\Delta H_{melting}$ where the bond can be easily break when expose to heat.

3.6 Postsynthetic Metathesis Monitored by PXRD

This topic was inspired by the literature precedent (Caira *et al*., 1995). When crystals of salt **1** were ground with various quantities of PIP, no significant changes were evident in the measured PXRD patterns. Piperazine is hygroscopic and can be transformed rapidly into a liquid/amorphous state under ambient conditions. This could be a factor as has been noted by Braga, Grepioni and Lampronti. (Braga *et al*., 2011) in their supramolecular metathesis experiments with isomeric tartaric acids and pyrazine which was noted to readily sublime. Apparently, when DABCO was ground with crystals of salt **2**, the PXRD indicated that partial supramolecular metathesis had occurred as the peculiar PXRD pattern of crystal salt **1** appeared. Hence, a series of dry grinding experiments were conducted in order to observe quantitatively where crystals of salt **2** were ground with 0.1 stoichiometric increments of DABCO. These experiments were perfectly reproducible and the same results were obtained when salt **2** was synthesised in powder form by grinding rather than as powdered single crystals.

Allied PXRD experiments were conducted where STL was co-ground with one molar equivalent of PIP and *n* equivalents of DABCO, with *n* varying in increments of 0.1 up to 1. Even when *n* was as low as 0.3 for DABCO, 26% of the sample comprised of salt **1** and this trend was maintained throughout the experiment, a clear preference for the formation of salt **1** over salt **2** was demonstrated in Figure 3.16.

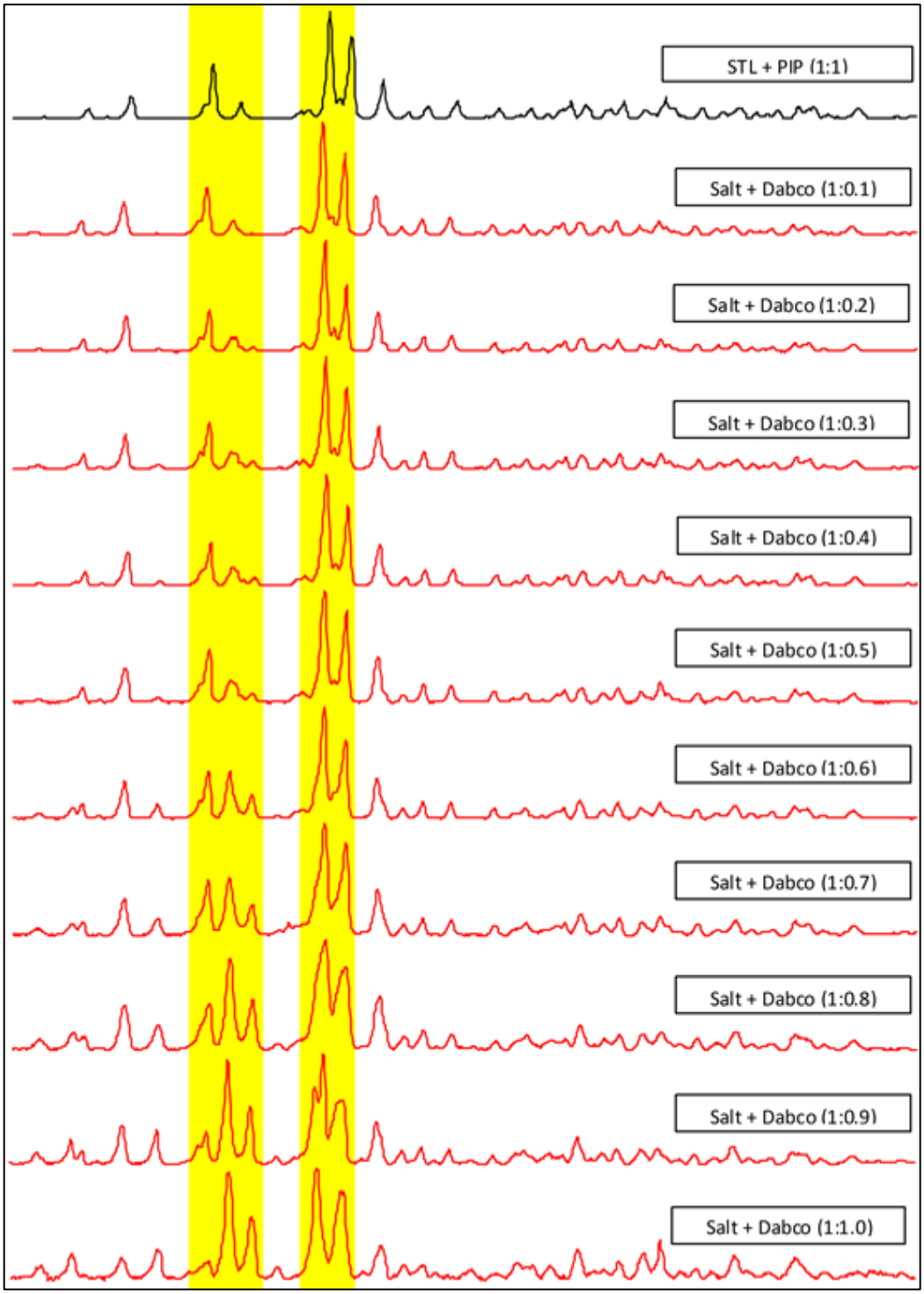

Figure 3.13: PXRD patterns when Salt **2** was ground (dry grinding) with 0.1–1.0 equivalents of DABCO

Table 3.8: Percentage of Salt **1** formed from addition of DABCO into Salt **2**

Mole equivalent of DABCO added to Salt 2	**Percentage of Salt 1 formed**
0.1	1.7
0.2	15.6
0.3	15.6
04	16.3
0.5	15.0
0.6	37.4
0.7	44.7
0.8	53.1
0.9	60.0
1.0	70.2

As shown in Figure 3.13 and Table 3.8, after 0.3 or more equivalents of DABCO were added, Rietveld refinement (Almelo, 2009) indicates that the conversion increased to a maximum of 70% after one molar equivalent was added.

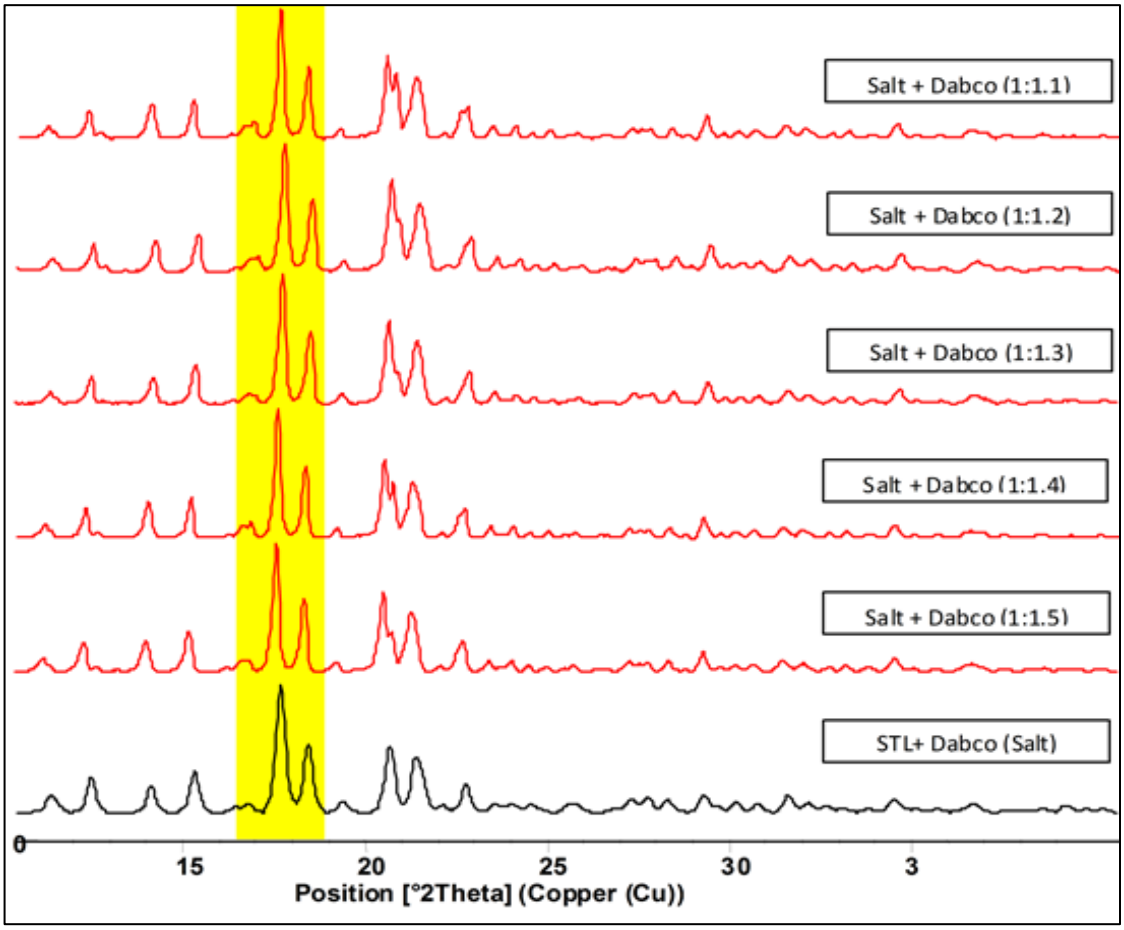

Figure 3.14: PXRD patterns when Salt **2** underwent LAG (ethanol) with 1.1–1.5 equivalents of DABCO

Table 3.9: Percentage of Salt **1** formed from LAG (using ethanol)

Mole equivalent of DABCO added to Salt 2	Percentage of Salt 1 formed
1.1	95.0
1.2	96.2
1.3	97.4
1.4	99.5
1.5	99.5

As shown in Figure 3.14 and Table 3.9, after addition of 1.4 equivalents of DABCO to salt **2** with a few drops of ethanol (LAG), quantitative conversion to salt **1** can be seen clearly with percentage of conversion of 99.5%.

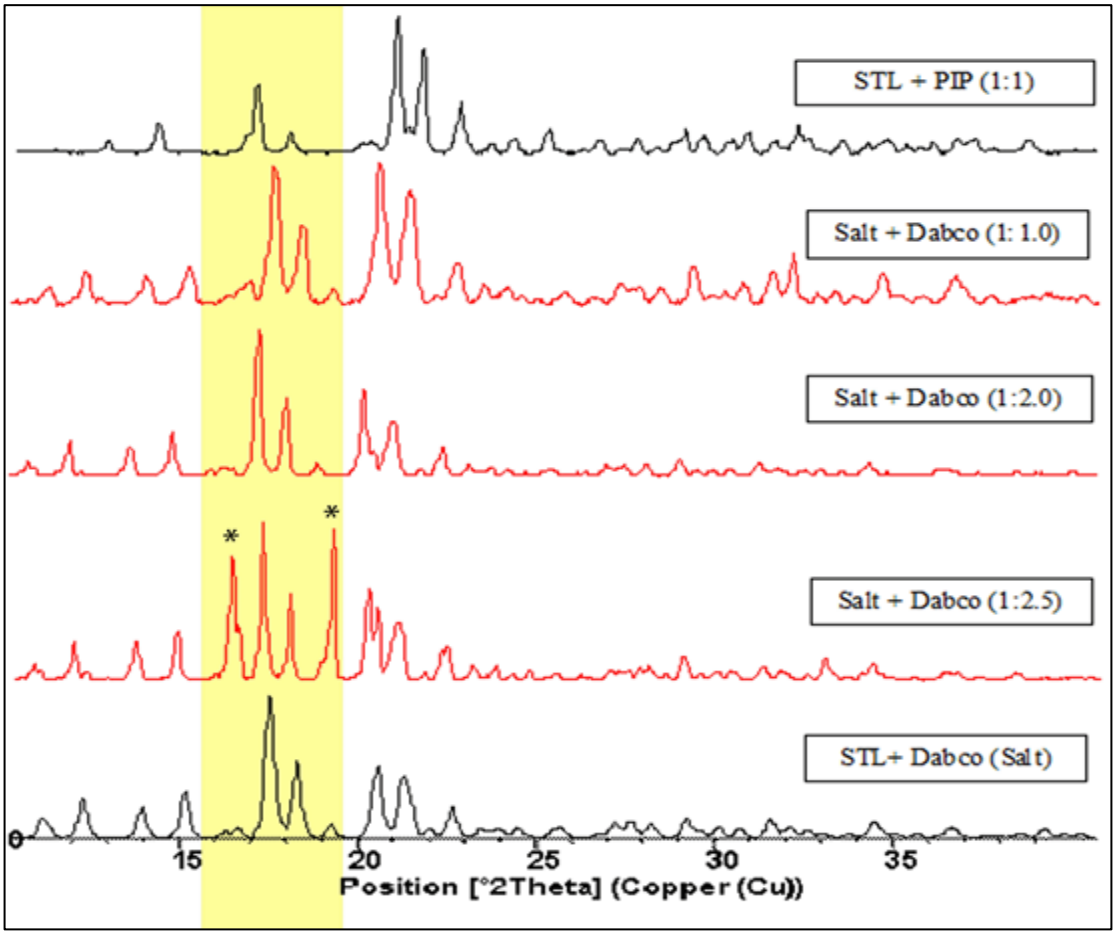

Figure 3.15: PXRD patterns when Salt **2** was ground (dry grinding) with 1.0, 1.5 and 2.5 equivalents of DABCO

From Table 3.8, at 1.0 molar equivalent of DABCO addition, the conversion to salt **1** was 70.2%, while at 2.0 molar equivalents, conversion to salt **1** was 93.0%. From figure 3.15, at 2.5 molar equivalents, the percentage of conversion rose to 97.6% with peaks assignable to unreacted DABCO, marked with asterisks were clearly evident in Figure 3.15.

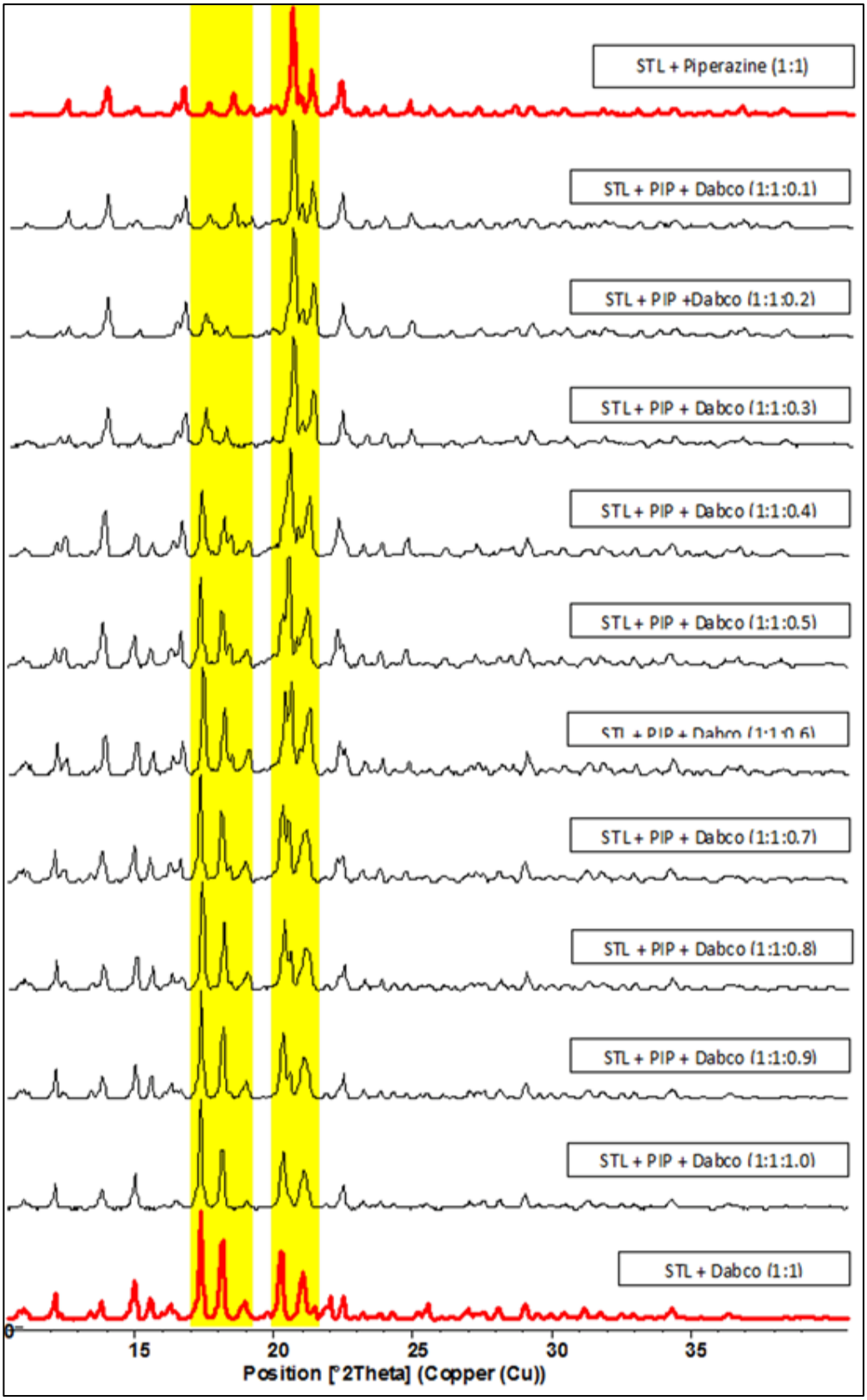

Figure 3.16: PXRD patterns when STL and PIP were ground with 0.1–1.0 equivalents of DABCO followed by dry grinding

Table 3.10: Percentage of Salt **1** formed when STL and PIP were ground with 0.1–1.0 equivalents of DABCO followed by dry grinding

Mole equivalent of DABCO added to 1:1 STL and PIP	Percentage of salt 1 formed
0.1	4.2
0.2	15.7
0.3	25.9
0.4	38.6
0.5	47.4
0.6	57.6
0.7	68.3
0.8	76.1
0.9	83.1
1.0	98.8

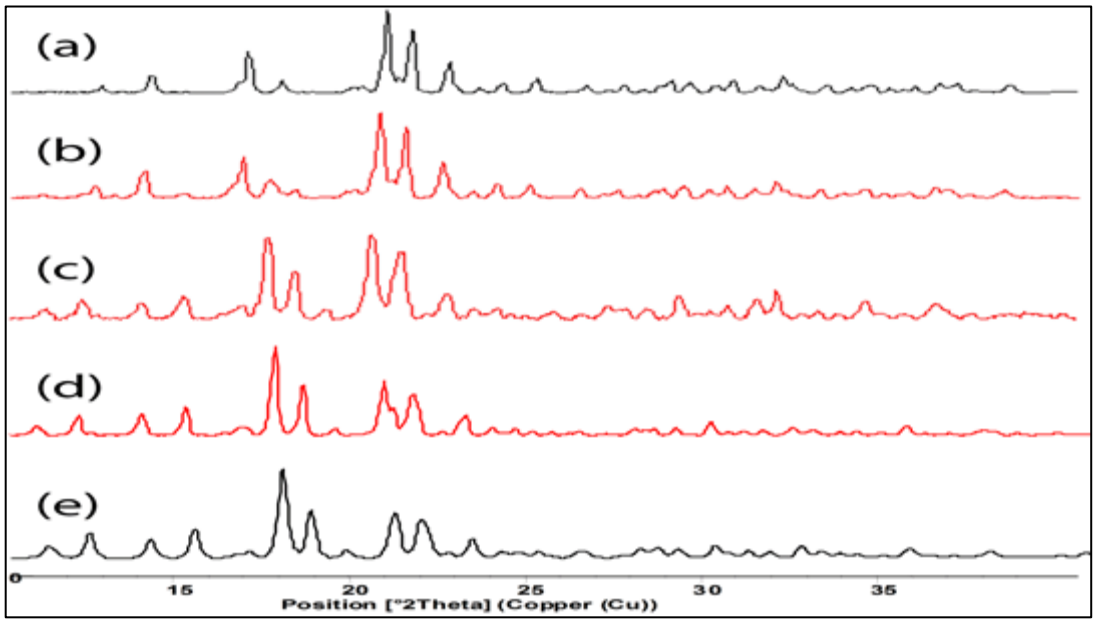

Figure 3.17: Representative of PXRD profiles

a. Ground crystals of salt **2**
b. Ground crystals of salt **2** with 0.5 molar equivalents of DABCO
c. Ground crystals of salt **2** with 1.0 molar equivalents of DABCO
d. Ground crystals of salt **2** with 1.5 molar equivalents of DABCO after LAG with ethanol
e. Ground crystals of salt **1**

Figure 3.17 shows representative PXRD profiles (relative intensity versus 2-Theta), traces shown in (b) and (c) show partial supramolecular metathesis up to a maximum of 70% in (c), and quantitative substitution in (d) yielding salt **1**, with the aid of LAG (ethanol). From Table 3.10, percentage of salt **1** formed when STL and PIP were ground with 0.1–1.0 equivalents of DABCO followed by dry grinding shows the preferential of formation of salt **1** over salt **2**.

A comparison of the hydrogen bonding in each structure provides a clue as to why the transformation of salt **2** to salt **1** occurs. With more acidic hydrogen atoms in salt **2** and therefore more conventional hydrogen bonds, two structural consequences occur. Crucially in salt **2**, with hydrogen bonds occurring between cations, absent in salt **1**, the layers are squeezed into a zigzag topology as opposed to the undulating layers in salt **1**. This projects the sulfanyl-O_1 atoms out of plane so these atoms do not form hydrogen bonds. The sulfanyl-O_1 atoms are therefore accessible for interaction with incoming DABCO upon grinding experiments with salt **2**. The driving force for the exchange is related to the observation that the aniline-N–H…O(sulfanyl) hydrogen bonds involving the bifurcated O_2 in salt **2** are systematically longer and weaker than the analogous hydrogen bonds in salt **1**, where each sulfanyl-O atom forms a strong aniline-N–H…O(sulfanyl) hydrogen bond. These structural differences along with the propensity of PIP to sublime combine to give a plausible explanation for the progress of the post synthetic metathetical reaction.

CHAPTER 4: CONCLUSION

Facile salt formation indicated in solution for STL and each of DABCO and PIP is vindicated by solution and dry grinding experiments. Even though the layered crystal structures of salt **1** and salt **2** are similar, salt **1** exhibits more efficient crystal packing, corroborated by packing efficiency calculations and DSC. This observation allows solid state postsynthetic metathesis where DABCO can displace PIP in salt **2** to form salt **1**. Such metathetical reactions are rare for organic compounds (Braga *et al*., 2011; Caira *et al*., 1995)' and the present study demonstrates that these can be conducted for salts as well as for species comprising neutral components. Further investigations into this phenomenon are underway.

Through the study of crystal engineering, the efficacy of this organic compound which has five solvent-free polymorphs and has proven to be capable of forming co-crystals with other sulfa drugs can be in enhanced. Formerly, sulfathiazole (STL) was widely used as a common oral and topical antimicrobial until it became ineffective due to growing of microbial resistance as a result of the use of antibiotics. However, sulfathiazole can be combined with other active pharmaceutical ingredients to form a new co-crystal salt with potential chemotherapeutic benefits.

REFERENCES

Aakeröy, C. B., Forbes, S., & Desper, J. (2014). Altering physical properties of pharmaceutical co-crystals in a systematic manner. *CrystEngComm*, *16*(26), 5870–5877.

Aakeröy, C. B., & Salmon, D. J. (2005). Building co-crystals with molecular sense and supramolecular sensibility. *CrystEngComm*, *7*(72), 439–448.

Advanced Chemistry Development (ACD/Laboratories). (2014). [computer software]. ACD/Laboratories: Toronto, Ontario, Canada.

Ali, H. R. H., Edwards, H. G. M., & Scowen, I. J. (2009). Insight into thermally induced solid-state polymorphic transformation of sulfathiazole using simultaneous in situ Raman spectroscopy and differential scanning calorimetry. *Journal of Raman Spectroscopy*, *40*(8), 887–892.

Almarsson, O., & Zaworotko, M. J. (2004). Crystal engineering of the composition of pharmaceutical phases. Do pharmaceutical co-crystals represent a new path to improved medicines? *Chemical Communications*, (17), 1889–1896.

Almelo, B. V. (2009). X'Pert HighScore Plus. PANalytical. [computer software]. The Netherlands.

Basics of X-Ray Diffraction: Diffraction spectra (1999). Retrieved from http://www.geo.umass.edu/courses/geo311/xrdbasics.pdf.

Boese, R., Kirchner, M. T., Billups, W. E., & Norman, L. R. (2003). Cocrystallization with acetylene: molecular complexes with acetone and dimethyl sulfoxide. *Angewandte Chemie International Edition*, *42*(17), 1961–1963.

Braga, D., Grepioni, F., & Lampronti, G. I. (2011). Supramolecular metathesis: co-former exchange in co-crystals of pyrazine with (R, R)-,(S, S)-,(R, S)-and (S, S/R, R)-tartaric acid. *CrystEngComm*, *13*(9), 3122–3124.

Brittain, H. G. (2009). Vibrational Spectroscopic Studies of Cocrystals and Salts. 2. The Benzylamine− Benzoic Acid System. *Crystal Growth & Design*, *9*(8), 3497–3503.

Caira, M. R. (2007). Sulfa drugs as model cocrystal formers. *Molecular Pharmaceutics*, *4*(3), 310–6.

Caira, M. R., Nassimbeni, L. R., & Wildervanck, A. F. (1995). Selective formation of hydrogen bonded cocrystals between a sulfonamide and aromatic carboxylic acids in the solid state. *Journal of the Chemical Society, Perkin Transactions 2*, (12), 2213.

Chierotti, M. R., Gaglioti, K., Gobetto, R., Braga, D., Grepioni, F., & Maini, L. (2013). From molecular crystals to salt co-crystals of barbituric acid via the carbonate ion and an improvement of the solid state properties. *CrystEngComm*, *15*(37), 7598–7605.

Coupar, P. I., Ferguson, G., & Glidewell, C. (1996). Piperazine–4, 4'-Sulfonyldiphenol (1/2): a Self-Assembled Channel Structure. *Acta Crystallographica Section C: Crystal Structure Communications*, *52*(12), 3052–3055.

Desiraju, G. R. (1989). *Crystal Engineering: The Design of Organic Solids* (1st ed.). Amsterdam: Elsevier Science.

Drebushchak, T. N., Boldyreva, E. V, & Mikhailenko, M. A. (2008). Crystal structures of sulfathiazole polymorphs in the temperature range 100–295 K: A comparative analysis. *Journal of Structural Chemistry*, *49*(1), 84–94.

Elder, D. P., Holm, R., & de Diego, H. L. (2013). Use of pharmaceutical salts and cocrystals to address the issue of poor solubility. *International Journal of Pharmaceutics*, *453*(1), 88–100.

Farrugia, L. J. (2012). WinGX and ORTEP for Windows: an update. *Journal of Applied Crystallography*, *45*(4), 849–854.

Flack, H. D. (1983). On Enantiomorph-Polarity Estimation. *Acta Crystallographica Section A: Foundations of Crystallography*, *39*(6), 876–881.

Friščić, T., & Jones, W. (2010). Benefits of cocrystallisation in pharmaceutical materials science: an update. *Journal of Pharmacy and Pharmacology*, *62*(11), 1547–1559.

Gelbrich, T., Hughes, D. S., Hursthouse, M. B., & Threlfall, T. L. (2008). Packing similarity in polymorphs of sulfathiazole. *CrystEngComm*, *10*(10), 1328.

Glusker, J. P., & Trueblood, K. N. (2010). *Crystal Structure Analysis: A Primer (IUCr Texts on Crystallography)*. Oxford University Press, USA.

Goud, N. R., Khan, R. A., & Nangia, A. (2014). Modulating the solubility of sulfacetamide by means of cocrystals. *CrystEngComm*, *16*(26), 5859–5869.

Grove, D. C., & Keenan, G. L. (1941). The Dimorphism of Sulfathiazole. *Journal of the American Chemical Society*, *63*(1), 97–99.

Higashi, T. (1995). *ABSCOR* [computer software]. Rigaku Corporation, Tokyo, Japan.

Hu, Y., Erxleben, A., Hodnett, B. K., Li, B., McArdle, P., Rasmuson, Å. C., & Ryder, A. G. (2013). Solid-State Transformations of Sulfathiazole Polymorphs: The Effects of Milling and Humidity. *Crystal Growth & Design*, *13*(8), 3404–3413.

Hu, Y., Erxleben, A., Ryder, A. G., & McArdle, P. (2010). Quantitative analysis of sulfathiazole polymorphs in ternary mixtures by attenuated total reflectance infrared, near-infrared and Raman spectroscopy. *Journal of Pharmaceutical and Biomedical Analysis*, *53*(3), 412–420.

Hu, Y., Gniado, K., Erxleben, A., & McArdle, P. (2014). Mechanochemical reaction of sulfathiazole with carboxylic acids: formation of a cocrystal, a salt, and coamorphous solids. *Crystal Growth & Design*, *14*(2), 803–813.

Kawakami, K. (2012). Modification of physicochemical characteristics of active pharmaceutical ingredients and application of supersaturatable dosage forms for improving bioavailability of poorly absorbed drugs. *Advanced Drug Delivery Reviews*, *64*(6), 480–495.

Kelleher, J. M., Lawrence, S. E., & Moynihan, H. A. (2006). Effect of the steric demand and hydrogen bonding capability of additives on the crystal polymorphism of sulfathiazole. *CrystEngComm*, *8*(4), 327.

Knop, O., Cameron, T. S., Bakshi, P. K., Linden, A., & Roe, S. P. (1994). Crystal chemistry of tetraradial species. Part 5. Interaction between cation lone pairs and phenyl groups in tetraphenylborates: crystal structures of Me3S+, Et3S+, Me3SO+, Ph2I+, and 1-azoniapropellane tetraphenylborates. *Canadian Journal of Chemistry*, *72*(8), 1870–1881.

Lawrence, S. E., McAuliffe, M. T., & Moynihan, H. A. (2010). Mimics of a R22(8) Hydrogen-Bond Dimer Motif: Synthesis and Influence on the Crystallisation of Sulfathiazole and Sulfapyridine. *European Journal of Organic Chemistry*, *2010*(6), 1134–1141.

Lee, I. S., Lee, A. Y., & Myerson, A. S. (2008). Concomitant polymorphism in confined environment. *Pharmaceutical Research*, *25*(4), 960–968.

Maddileti, D., Swapna, B., & Nangia, A. (2014). High solubility crystalline pharmaceutical Forms of blonanserin. *Crystal Growth & Design*, *14*(5), 2557–2570.

McArdle, P., Hu, Y., Lyons, A., & Dark, R. (2010). Predicting and understanding crystal morphology: the morphology of benzoic acid and the polymorphs of sulfathiazole. *CrystEngComm*, *12*(10), 3119.

Mcintosh, J., Robinson, R. H. M., & Selbie, F. R. (1945). Acridine-Sulphonamide Compounds as Wound Antiseptics Clinical Trials of Flavazole. *The Lancet*, *246*(6361), 97–99.

Moradiya, H., Islam, M. T., Woollam, G. R., Slipper, I. J., Halsey, S., Snowden, M. J., & Douroumis, D. (2013). Continuous Cocrystallization for Dissolution Rate Optimization of a Poorly Water-Soluble Drug. *Crystal Growth & Design*, *14*(1), 189–198.

Munroe, Á., Croker, D. M., Rasmuson, Å. C., & Hodnett, B. K. (2014). Solution-Mediated Polymorphic Transformation of FV Sulphathiazole. *Crystal Growth & Design*, *14*(7), 3466–3471.

Munroe, A., Croker, D., Rasmuson, Å. C., & Hodnett, B. K. (2011). Analysis of FII crystals of sulfathiazole: epitaxial growth of FII on FIV. *CrystEngComm*, *13*(3), 831–834.

Munroe, Á., Rasmuson, Å. C., Hodnett, B. K., & Croker, D. M. (2012). Relative Stabilities of the Five Polymorphs of Sulfathiazole. *Crystal Growth & Design*, *12*(6), 2825–2835.

Nakanishi, W., Nakamoto, T., Hayashi, S., Sasamori, T., & Tokitoh, N. (2007). Atoms-in-molecules analysis of extended hypervalent five-center, six-electron (5c-6e) C_2Z_2O interactions at the 1,8,9-positions of anthraquinone and 9-methoxyanthracene systems. *Chemistry - A European Journal*, *13*(1), 255–268.

Nangia, A. (2010). Supramolecular chemistry and crystal engineering. *Journal of Chemical Sciences*, *122*(3), 295–310.

Parkin, A., Collins, A., Gilmore, C. J., & Wilson, C. C. (2008). Using small molecule crystal structure data to obtain information about sulfonamide conformation. *Acta Crystallographica Section B: Structural Science*, *64*(1), 66–71.

Parmar, M. M., Khan, O., Seton, L., & Ford, J. L. (2007). Polymorph Selection with Morphology Control Using Solvents. *Crystal Growth & Design*, *7*(9), 1635–1642.

Rigaku/MSC inc. (2004). *CrystalClear User Manual*. Rigaku Corporation, Tokyo, Japan.

Roy, S., Chamberlin, B., & Matzger, A. J. (2013). Polymorph Discrimination Using Low Wavenumber Raman Spectroscopy. *Organic Process Research & Development*, *17*(7), 976–980.

Schultheiss, N., & Newman, A. (2009). Pharmaceutical Cocrystals and Their Physicochemical Properties. *Crystal Growth & Design*, *9*(6), 2950–2967.

Sekhon, B. S. (2012). Drug-drug co-crystals. *DARU Journal of Pharmaceutical Sciences*, *20*(1), 45.

Shan, N., & Zaworotko, M. J. (2008). The role of cocrystals in pharmaceutical science. *Drug Discovery Today*, *13*(9–10), 440–6.

Sheldrick, G. M. (2008). A short history of SHELX. *Acta Crystallographica Section A*, *64*(1), 112–122.

Sovago, I., Gutmann, M. J., Hill, J. G., Senn, H. M., Thomas, L. H., Wilson, C. C., & Farrugia, L. J. (2014). Experimental Electron Density and Neutron Diffraction Studies on the Polymorphs of Sulfathiazole. *Crystal Growth & Design*, *14*(3), 1227–1239.

Spek, A. L. (2003). Single-crystal structure validation with the program PLATON. *Journal of Applied Crystallography*, *36*(1), 7–13.

Stahl, P. H., & Wermuth, C. G. (2002). *Handbook of pharmaceutical salts: properties, selection, and use* (Vol. 2). Weinheim, Germany: Wiley-Vch.

Stahly, G. P. (2009). A Survey of Cocrystals Reported Prior to 2000. *Crystal Growth & Design*, *9*(10), 4212–4229.

Tilborg, A., Norberg, B., & Wouters, J. (2014). Pharmaceutical salts and cocrystals involving amino acids: a brief structural overview of the state-of-art. *European Journal of Medicinal Chemistry*, *74*, 411–426.

Trask, A. V, Motherwell, W. D. S., & Jones, W. (2004). Solvent-drop grinding: green polymorph control of cocrystallisation. *Chemical Communications*, *0*, 890–891.

Wright, P. M., Seiple, I. B., & Myers, A. G. (2014). The evolving role of chemical synthesis in antibacterial drug discovery. *Angewandte Chemie (International Ed. in English)*, *53*(34), 8840–69.

LIST OF PUBLICATIONS

Aznan, A. M. A., Abdullah, Z., Lee, V. S., & Tiekink, E. R. T. (2014). Crystal structure of a new monoclinic polymorph of N-(4-methylphenyl)-3- nitropyridin-2-amine. *Acta Crystallographica Section E: Structure Reports Online*, *70*(8), 58–61.

Aznan, A. M. A., Abdullah, Z., Khoo, C. H., Chen, B. J., See, T. H., Sim, J. H., … Tiekink, E. R. T. (2015). Three ammonium salts of sulfathiazole: Crystallography and anti-microbial assay. *Zeitschrift Fur Kristallographie - Crystalline Materials*, *230*(6), 385–396.

Aznan, A. M. A., Safwan, A. P., Abdullah, Z., Kaulgud, T., Arman, H. D., … Tiekink, E. R. T. (2014). Postsynthetic Metathesis in an All Organic Two-Dimensional Array Mediated by Hydrogen Bonding. *Crystal Growth & Design*, *14*, 5794–5800.

LIST OF PRESENTATIONS

Dalton 2014 Conference, "Supramolecular Methathesis: cation exchange in salts derived from the sulfa-drug, Sulfathiazole", Poster presentation (International), 15-17 April 2014, University of Warwick, Coventry, England.

5 th UM-NUS-CU Trilateral Mini Symposium and Scientific Meeting 2014, "Supramolecular Methathesis: cation exchange in salts derived from the sulfa-drug, Sulfathiazole", Poster presentation (International), 11-12 February 2014, University of Malaya, Kuala Lumpur, Malaysia.

University of Malaya Chemical Crystallography Symposium 2014, "Supramolecular Methathesis: cation exchange in salts derived from the sulfa-drug, Sulfathiazole", Poster and oral presentation (National), 28 May 2014, University of Malaya, Kuala Lumpur, Malaysia.

University of Malaya Pharmaceutical Co-Crystal Symposium 2014, "Supramolecular Methathesis: cation exchange in salts derived from the sulfa-drug, Sulfathiazole", Poster and oral presentation (National), 19 July 2014, University of Malaya, Kuala Lumpur, Malaysia.

APPENDIX

APPENDIX A: ^{1}H NMR and IR

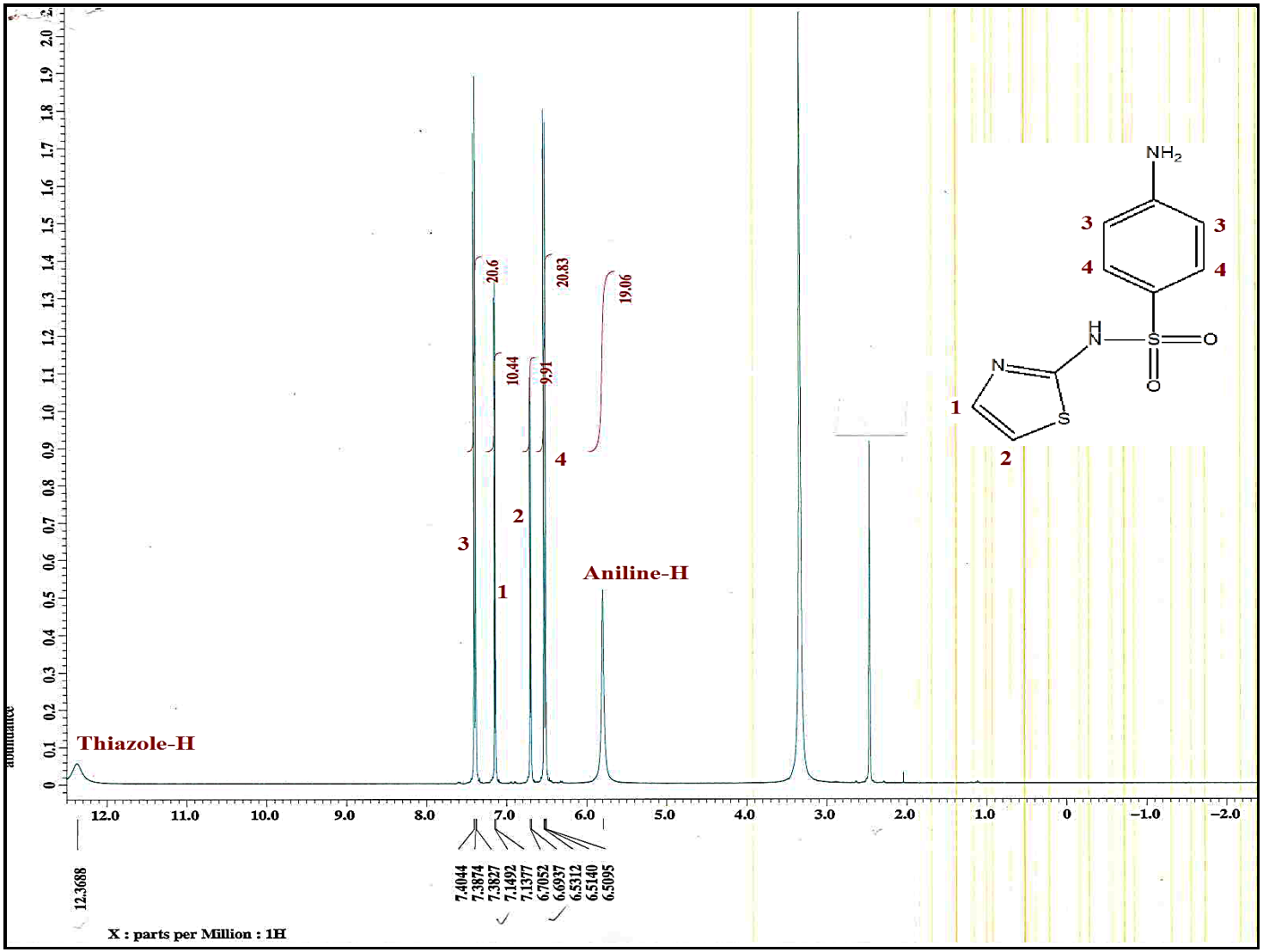

^{1}H NMR Spectrum (DMSO-d_6, 400 MHz) of Sulfathiazole

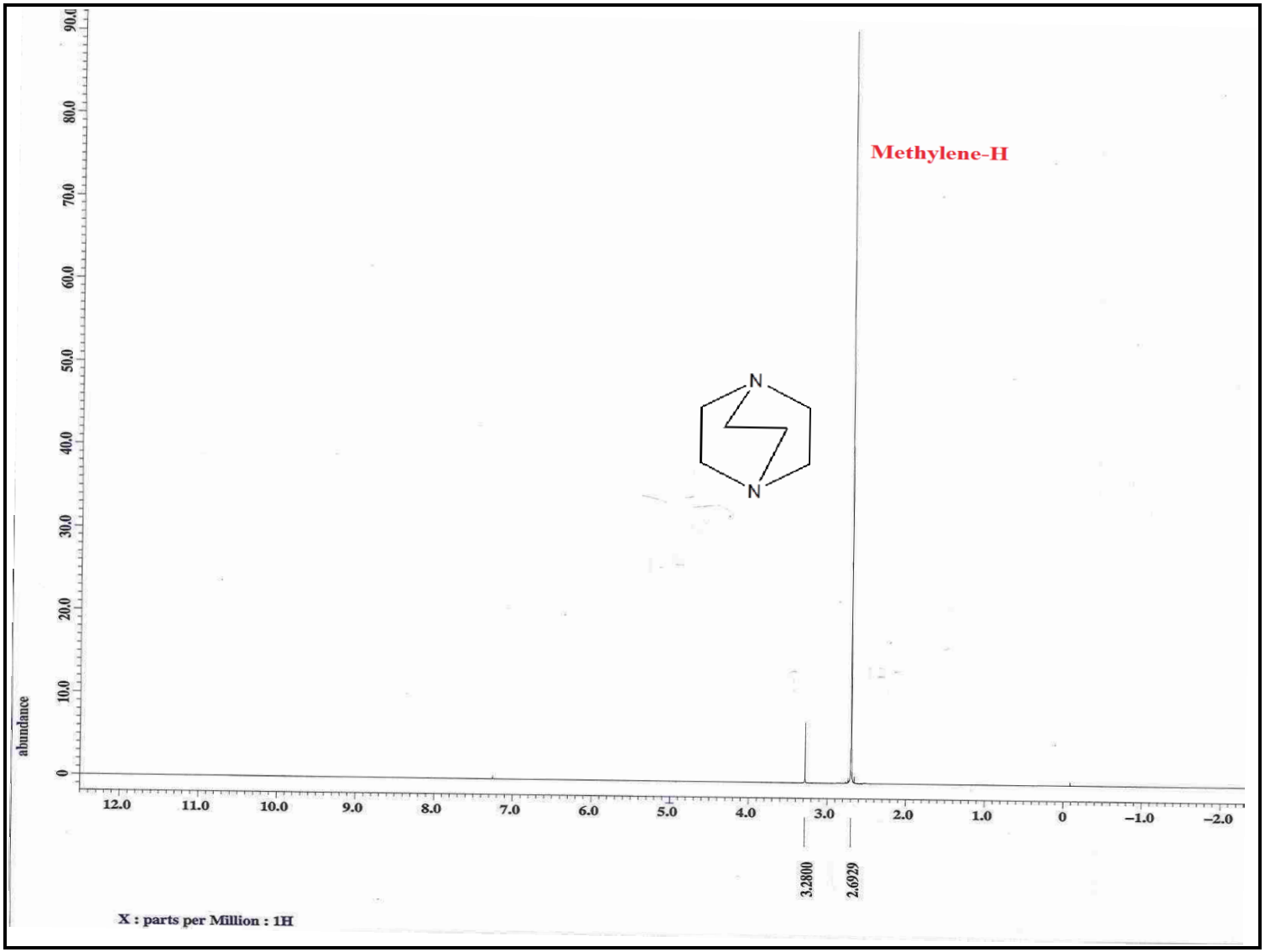

^{1}H NMR Spectrum (DMSO-d_6, 400 MHz) of DABCO

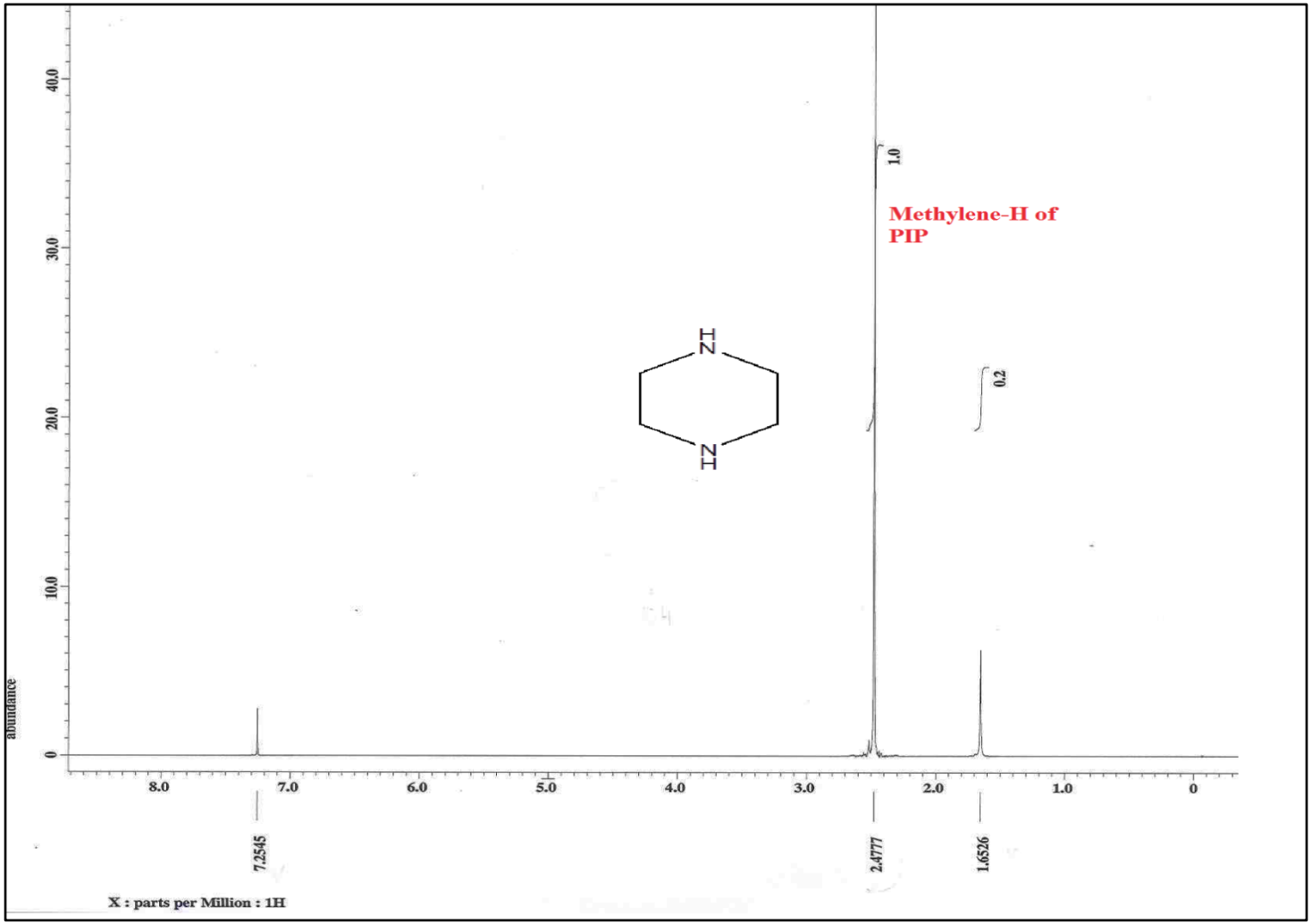

^{1}H NMR Spectrum (DMSO-d_6, 400 MHz) of Piperazine

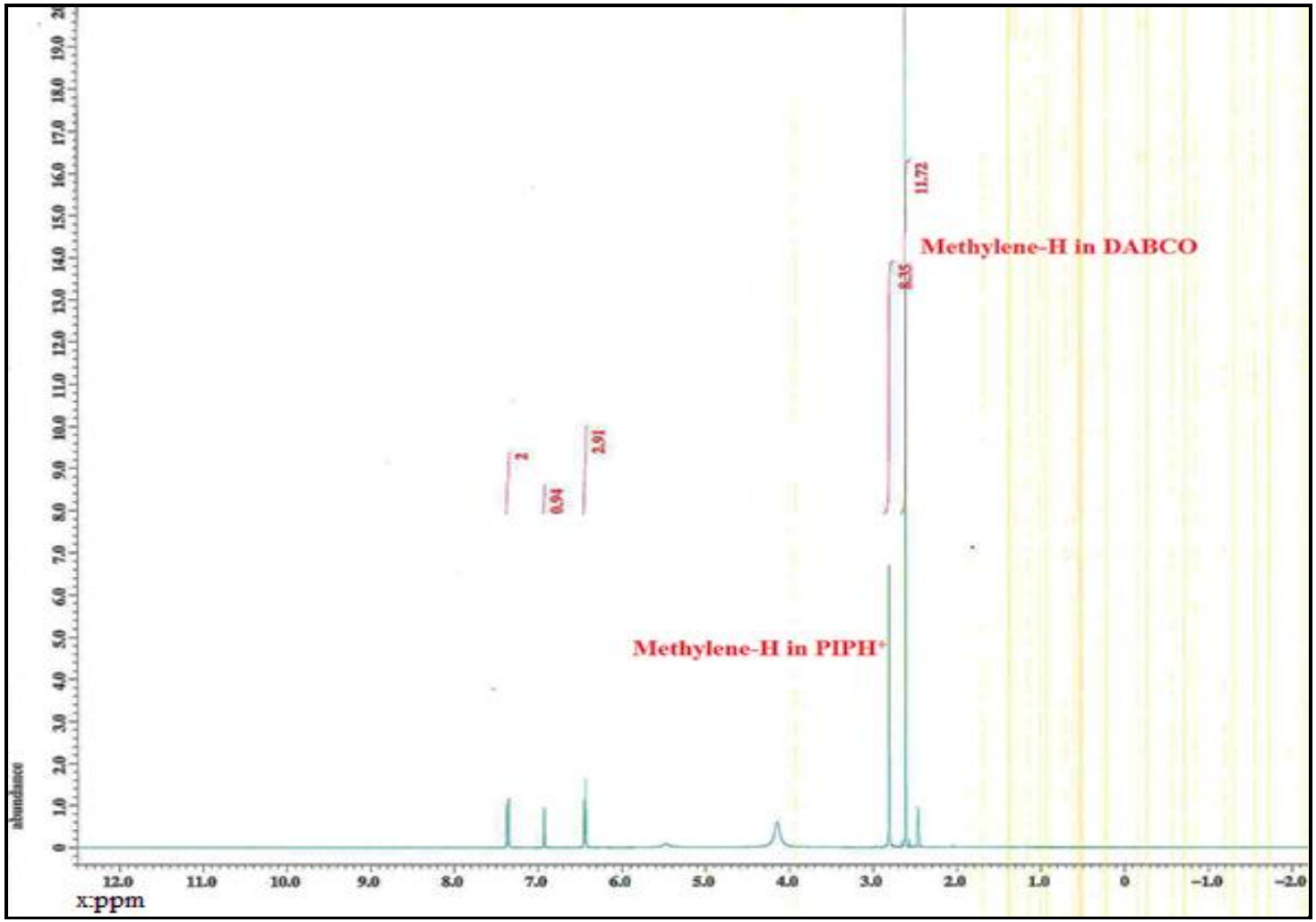

^{1}H NMR Spectrum (DMSO-d_6, 400 MHz) of STL, DABCO & PIP

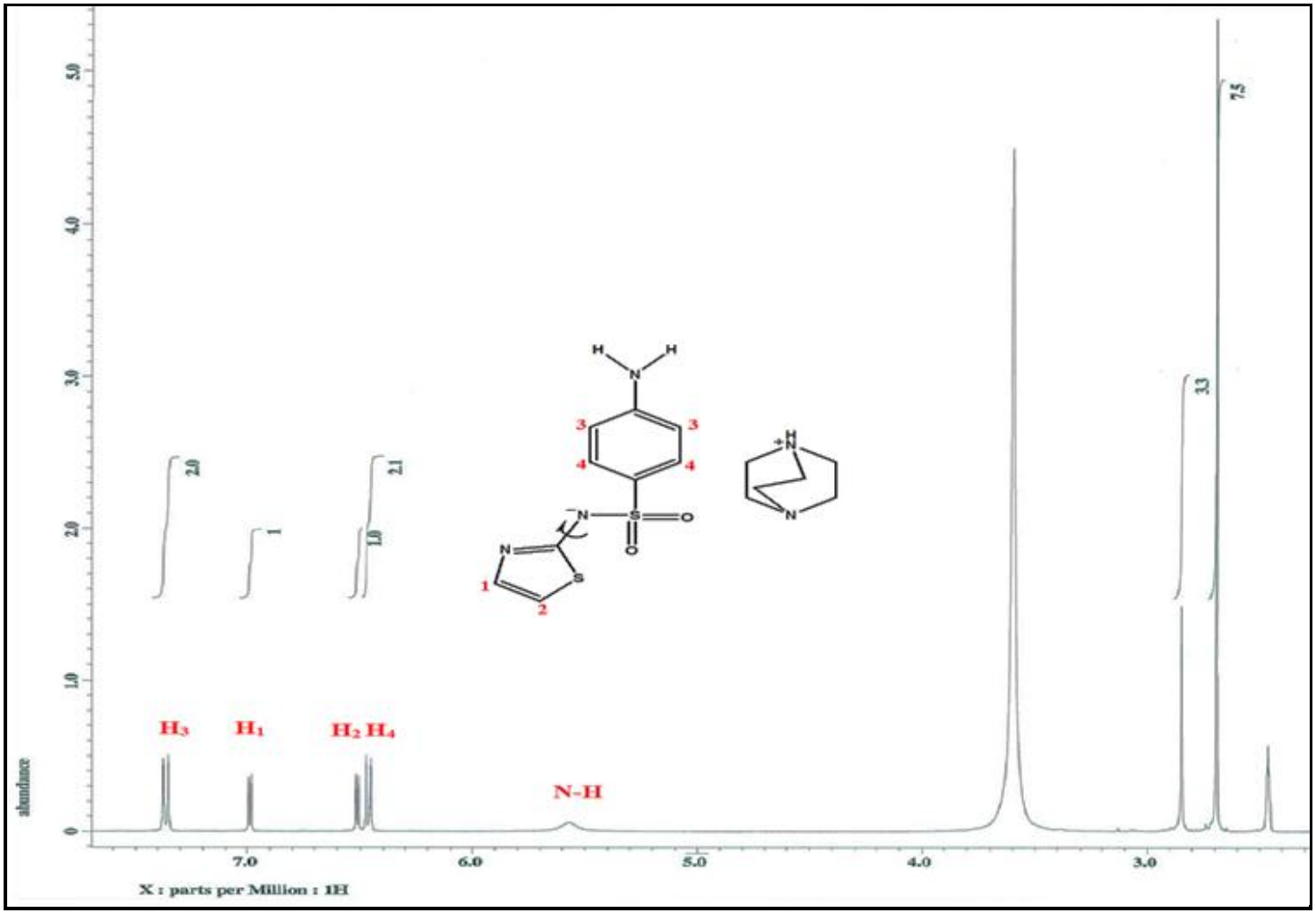

^{1}H NMR Spectrum (DMSO-$d_{6,}$ 400 MHz) of Salt 1, [DABCOH][STL_H]

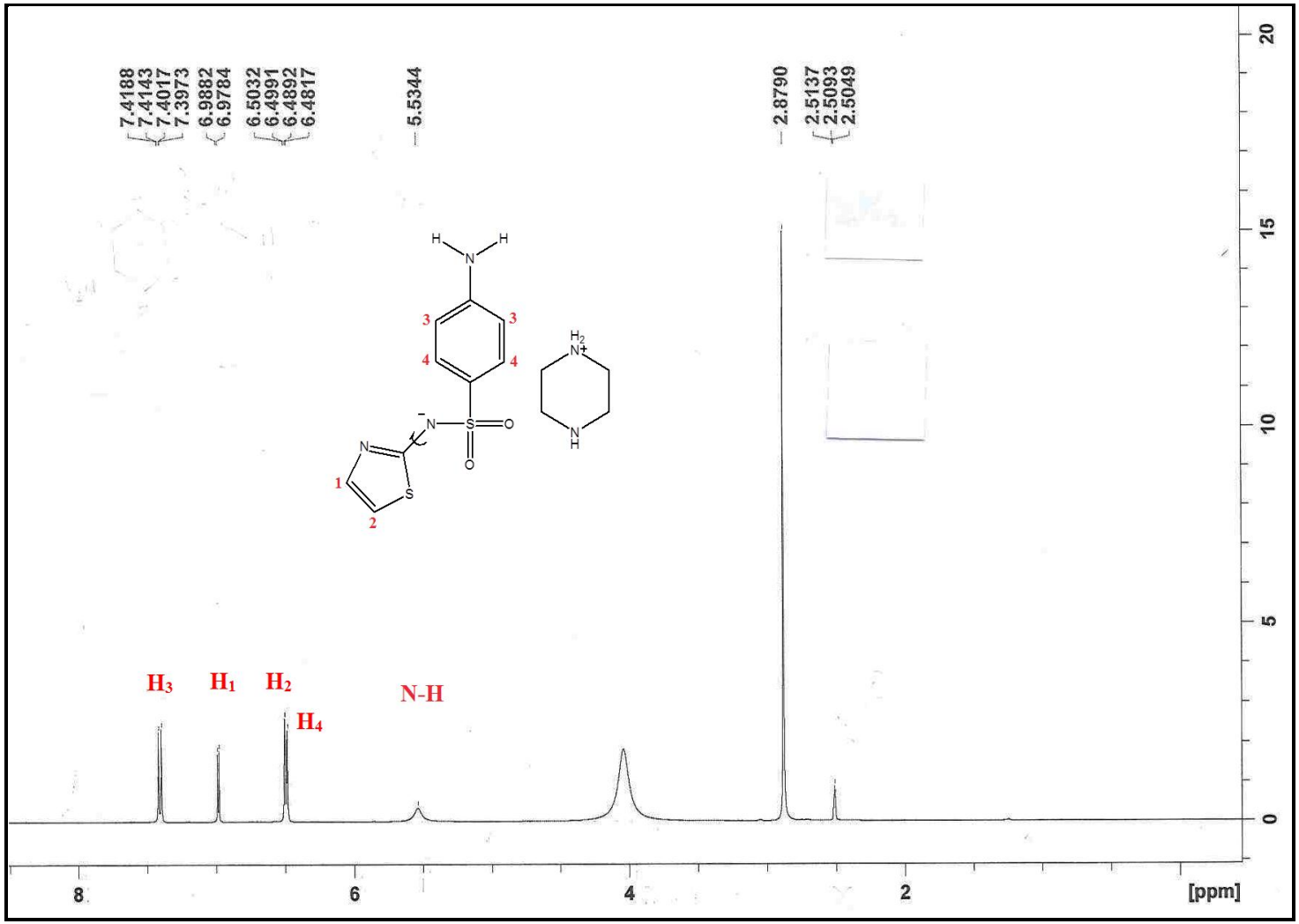

^{1}H NMR Spectrum (DMSO-d_6, 400 MHz) of Salt 2, [PIPH][STL_H]

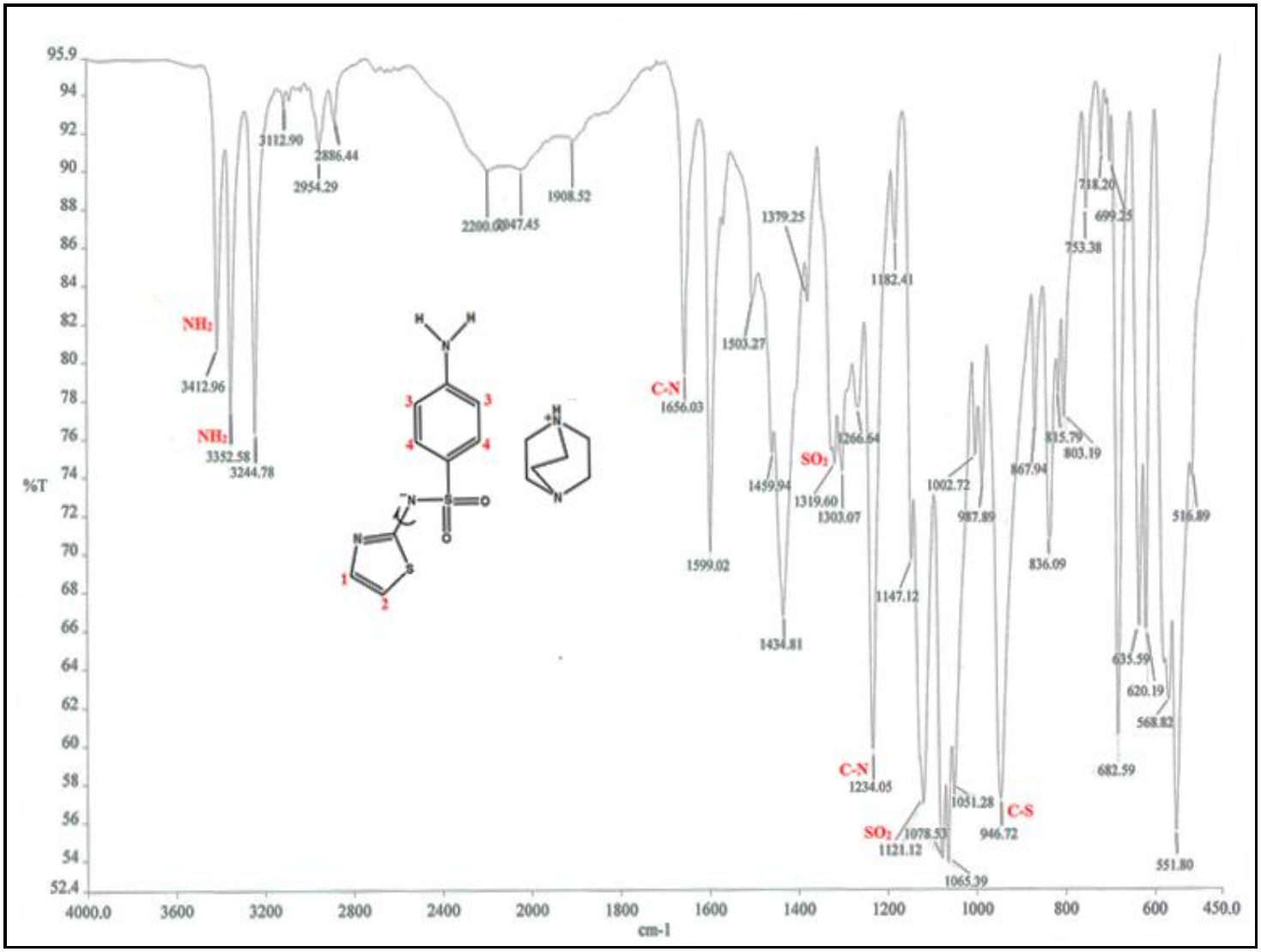

IR Spectrum of Salt 1, [DABCOH][STL_H]